

DELFT UNIVERSITY OF TECHNOLOGY

FACULTY OF AEROSPACE ENGINEERING

AE2111-I

AEROSPACE SYSTEMS DESIGN

Design of the JUICE Spacecraft

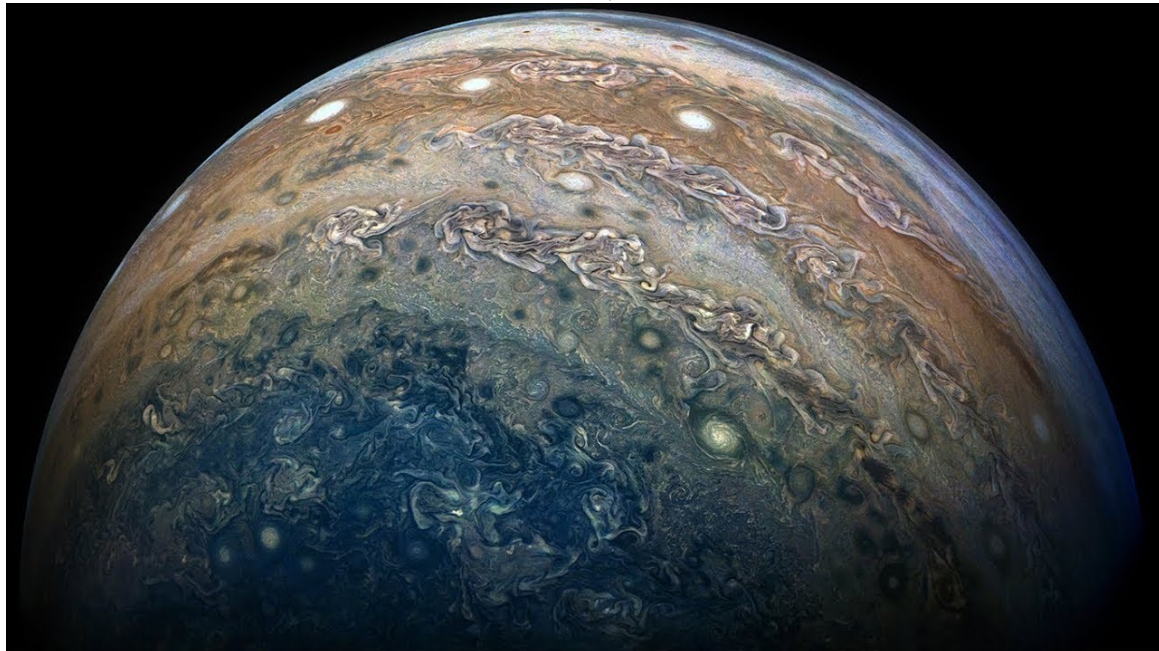
A Mission to the Giant of our Solar Systems

Mission: Jupiter's JUICE mission

Lecturer: W.A. Timmer

Teaching Assistant: Lidia Rzeplińska

March 29, 2022



Group B11

Antonio Minafra	5027993	Sam Broos	4992873
Jonatan Valk	5028817	Silvano Tromp	5049237
Niklas Knöll	5006961	Stefano Kok	4656091
Lorenz Veithen	5075211	Tarek Abdelrazek	4993004

Summary

In previous work packages a mission to study Jupiter is described and the subsystems have been designed. For this mission it is very important that the instruments can make accurate measurements. One of these subsystems, the attitude determination and control system, is very important to make sure this is possible. The subsystem is studied and designed in further detail.

First, sensors and actuators are identified and compared. Secondly, the disturbance torques acting on the spacecraft are investigated. From calculations it is found that an external disturbance torque of $9.558 \cdot 10^{-4}$ Nm acts on the spacecraft in the heliocentric orbit. From this value it is determined that torque that has be able to be provided by the momentum wheel is 2.867 mNm. In the model fuel loads and sloshing is neglected. Sloshing can be minimized by introducing baffles and bladders, a period to allow the fuel to settle, small changes in angular velocity to avoid fluid excitation and notch filters.

Subsequently, multiple actuator and sensor configurations generated. These configurations are compared with each other and the best actuator and sensor configuration is selected. The actuator configuration chosen uses four momentum wheels and thrusters. The configuration uses four reaction wheels and thrusters to add redundancy, this prevents a single point of failure. Momentum wheels allow the spacecraft to perform all ADCS manoeuvres and provide gyroscopic stiffness. Thrusters are required for momentum dumping, which builds up in the reaction wheels. The sensor configuration chosen uses three coarse sun sensors, two star sensors and six gyroscopes. The star sensors provide high accuracy attitude determination for the spacecraft, two sensors are used for redundancy. For higher angular velocities three sun sensors can provide less accurate attitude determination for de-tumbling of the spacecraft. Finally the configurations uses two sets of three gyroscopes for redundancy. Therefore, this is a very failure resistant configuration. Finally the attitude determination and control system is integrated into the spacecraft. The power consumption of the sensors and actuators are summarized in the following Table.

Table 1: Power consumption of sensors and actuators

Sensor or actuator	Power [W]	Voltage [V]	Current [A]
Coarse Sun sensor (x3)	0	0-0.09	0.035
ASTRO APS	<12	30-52	-
VST-68M	3	9-40	-
ASTRIX 1120 (x2)	13.5	22-50	-
RSI 15-215/20 (x4)	15	21 to 37	< 4.5
RMR-106F 40N (x4)	20.1	28	-

An overview of how the subsystem is integrated is given in the following diagram.

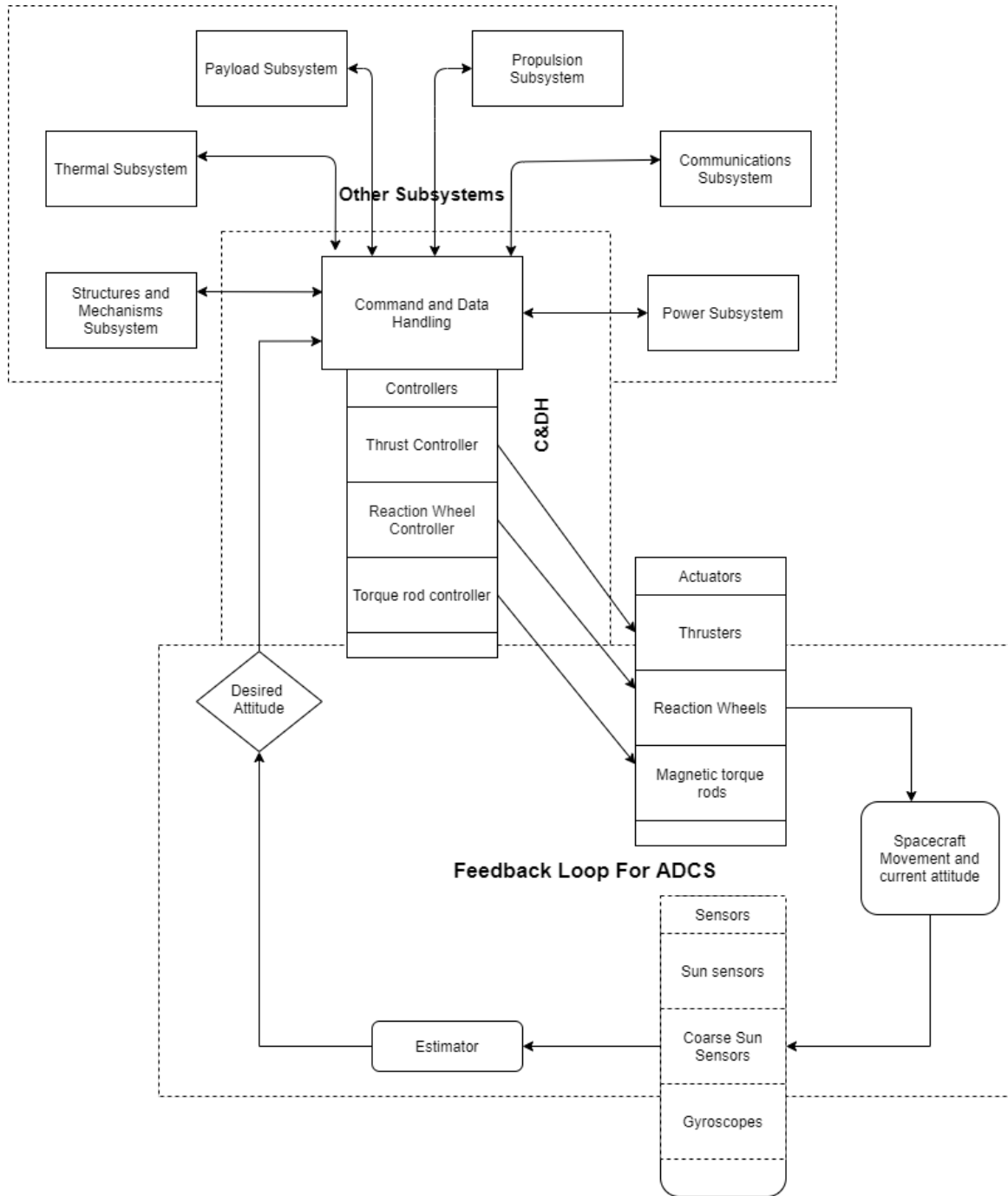


Figure 1: ADCS architecture diagram

List of Symbols

Latin Letters	Quantity	Symbol Unit
a	Semi-major axis	km
A	Cross sectional rea	m^2
\vec{B}	Magnetic field	T
\vec{D}	Dipole moment	Am^2
\vec{M}	Torque	Nm
I	Current	A
P	Power	W
R	Resistance	Ω
T_D	Disturbance torque	Nm
T_{RW}	Required torque of the wheel	Nm
V	Voltage	V

Greek Letters	Quantity	Symbol Unit
α	Absorptivity	
η	Efficiency	[·]
ϵ_{IR}	Infrared emissivity	[·]
μ	Standard gravitational parameter	km^3/s^2
μ_{BAT}	Battery efficiency	[·]
ρ_r	Reflectivity	[·]
σ	Boltzmann constant	[·]

List of Figures

1	ADCS architecture diagram	ii
2.1	Bradford Coarse Sun Sensor	2
2.2	Bradford Fine Sun Sensor	3
2.3	Sodern STD 15	3
2.4	Jena Optronik ASTRO APS	4
2.5	Vectronic Aerospace VST-41M	4
2.6	ASTRIX 1120	5
2.7	CIRUS-EX	5
2.8	MRM-106F [10]	6
2.9	MRM-122 130N [10]	6
2.10	MONARC-5 [11]	6
2.11	Reaction/momentum wheel from Collins Aerospace	7
2.12	Representation of the control moment gyro [13]	8
2.13	Magnetorquer example (QT-40)	8
2.14	Timeline of the mission with important ADCS modes	9
2.15	Axis system used	10
2.16	Center of Mass	11
2.17	Dimensions for center of pressure in [m]	12
3.1	The Side of JUICE facing Jupiter	21
3.2	Initial view of the Spacecraft in model	22
3.3	Initial View of the Momentum Wheels in model	22
3.4	Pyramid Momentum Wheel Configuration [13]	22
4.1	ADCS architecture diagram	27
A.1	Configuration S1 and A1	.
A.2	Configuration S3 and A2	.
A.3	Configuration S2 and A1	.
A.4	Configuration S4 and A3	.

List of Tables

1	Power consumption of sensors and actuators	i
2.1	Specifications of Bradford CSS [1]	2
2.2	Specifications of Bradford FSS [2]	3
2.3	Specifications of Sodern STD 15 [3]	3
2.4	Specifications of ASTRO 15 and VST-68M [6] [5]	4
2.5	Specifications of ASTRO APS and VST-41M [4] [5]	4
2.6	Specifications of ASTRIX 1120 [8] and CIRUS-EX [9]	4
2.7	Specifications of RCS thrusters [aerojetrocketdyne2020 \cite {moog2018}]	6
2.8	Information about two momentum wheels from Collins Aerospace[12]	7
2.9	Control moment gyroscope from Airbus [14]	8
2.10	Example of a magnetorquer [15]	8
2.11	Center of mass calculations z axis	11
2.12	Disturbance torques	15
3.1	Trade off table for sensor configuration	20
3.2	Trade off table for actuator configuration	20
4.1	Types of sensors and actuators and their power consumption	26
5.1	Power consumption of sensors and actuators	28
A.1	Part list S1 and A1
A.2	Part list S3 and A2
A.3	Part list S2 and A1
A.4	Part list S4 and A3
B.1	Task distribution per member

List of Abbreviations

- ADCS - *Attitude Determination and Control System*
BOL - *Beginning of Life*
CDH - *Command and Data Handling*
CMG - *Control Moment Gyroscope*
DASML - *Delft Aerospace Structures and Materials Laboratory*
DOD - *Depth of discharge*
EPS - *Electrical and Power System*
EOL - *End of Life*
FAA - *Federal Aviation Administration*
HES - *High-efficiency silicon*
LEO - *Low Earth Orbit*
MMOI - *Mass moment of inertia*
PCDU - *Power control and distribution unit*
PCU - *Power conditioning and control unit*
PDU - *Power distribution unit*
RTG - *Radioisotope Thermoelectric Generator*
RCS - *Reaction Control System*
S/C - *Spacecraft*
TBD - *To be determined*
TJ - *Triple Junction TT&C - Telemetry, Tracking and Control*
TW - *Technical Writing* WP1 - *Workpackage 1*
WP2 - *Workpackage 2*

Contents

Summary	i
List of Figures	iv
List of Tables	v
1 Introduction	1
2 Subsystems Detail Design	2
2.1 Types of Sensors and Actuators	2
2.2 Torque and Control Effects of the Actuators	9
2.3 Possible Configurations of the Subsystem	16
3 Baseline Selection	19
3.1 Trade Off Criteria	19
3.2 Trade Off	20
3.3 CATIA Kinematic Model	21
4 Subsystem Integration	24
4.1 Integration of ADCS	24
4.2 ADCS interface	25
4.3 ADCS subsystem diagram	27
5 Conclusion	28
References	29
Appendix A CATIA Drawings	
A.1 Configuration S1 and A1
A.2 Configuration S3 and A2
A.3 Configuration S2 and A1 with the other Components
A.4 Configuration S4 and A3 with the other Components
Appendix B Task Distribution	

Introduction 1

In the history of mankind, humans gazed up to the sky and wondered what was up there. After the Sun, the Moon and Venus, Jupiter is the brightest object in the sky and can easily be recognized by the naked eye, as was already done by the Babylonian astronomers in the 7th or 8th century BC. Furthermore, Jupiter is by far the most massive planet in our solar system, being 318 times the mass Earth. However, only one spacecraft is currently orbiting the planet: Juno. To gain further scientific knowledge about the planet, and specifically its atmospheric phenomena, a mission to Jupiter is being developed for which the JUICE orbiter will be designed.

The aim for this report is to describe the design process for the Attitude Determination and Control Subsystem (ADCS) of the JUNO spacecraft. Firstly, the sensors and actuators available for use are going to be identified, then a detailed prediction of the torque the actuators, as well as various environmental disturbances have on the spacecraft will be made. Different possible configurations of sensors and actuators are going to be defined and traded-off, resulting in a final configuration. Finally, the chosen configuration of the ADCS will be explained, along with its integration with the rest of the spacecraft.

This report will have the following structure: in chapter 2 a detailed analysis of the ADCS will be done. The sensors and actuators will be investigated, the key properties shall be given and detailed predictions of the torque and control effects of the actuators will be done. In the end of chapter 2 various possible configurations will be presented. In chapter 3 the configurations of chapter 2 will be traded off with their advantages and disadvantages. In chapter 4 a detailed description of the integration of the ADCS with the spacecraft will be given and the design of the interface between the spacecraft and ADCS shall be explained. In the end, a detailed ADCS subsystem diagram will be provided.

Subsystems Detail Design **2**

This chapter aims to provide a more detailed analysis of the Attitude Determination and Control Subsystem (ADCS). This is done in several steps. First, three types of sensors and actuators are investigated as the main components of the ADCS in section 2.1, the key properties of each are then given for the different operation modes. In section 2.2, detailed calculations of the torque and control effects of the disturbances and actuators chosen are performed. Lastly, section 2.3 presents a variety of configurations of the subsystem based on the effects the actuators of the ADCS on the spacecraft and vice versa. The (dis)advantages of each are also investigated.

2.1 Types of Sensors and Actuators

In this section, the sensors and actuators of the ADCS are considered. For each type of sensor and actuator tables are given comparing the performance and specifications of multiple examples for each type.

2.1.1 ADCS Sensors

The determination of the current attitude relies on sensors that are placed on-board of the spacecraft. In this section, three such possibilities of sensors are investigated: coarse sun sensors, star sensors and gyroscopes.

Coarse Sun Sensor

Coarse sun sensors can provide a coarse measurement of the attitude with the sun as reference. As a trade off to their low precision and providing only one vector, they are very reliable and work at high rotation rates. As an example for typical specifications of this type of sensors, the Bradford Coarse Sun Sensor can be seen in Figure 2.1 and its specifications are listed in Table 2.1.

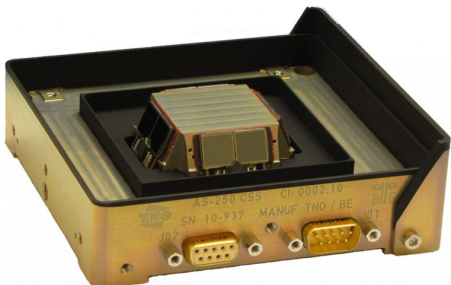


Figure 2.1: Bradford Coarse Sun Sensor

Table 2.1: Specifications of Bradford CSS [1]

Parameter	Value
Mass	215 g
Power	0 W
Size	110x110x30 mm
Data Interface	4 Analog channels 0 - 90 mV
Accuracy	<1.5 ° (3 σ)
Reliability	12 FIT @60 °C

Fine Sun Sensor

Fine sun sensors work quite similarly to coarse sun sensors, just with a better accuracy and a lower field of view. As an example for a typical sensor Bradford's FSS is shown in Figure 2.2 and its specifications are listed in Table 2.2



Figure 2.2: Bradford Fine Sun Sensor

Table 2.2: Specifications of Bradford FSS [2]

Parameter	Value
Mass	375 g
Power	<0.25 W
Size	108x108x52.5 mm
Data Interface	4 Analog channels 0 - 5 V
Accuracy	<0.03 ° or 108 arcsec (3 σ)
Reliability	70 FIT @30 °C

Earth/Horizon Sensor

Horizon sensors detect the horizon of the body they are orbiting, thus providing a reference direction. As they detect the horizon, they only work when in orbit around a body. The specifications of the scanning horizon sensor STD 15 is given in Table 2.3 and a picture of the sensor is shown in Figure 2.3.

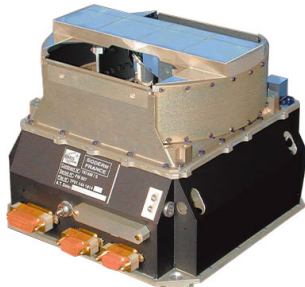


Figure 2.3: Sodern STD 15

Table 2.3: Specifications of Sodern STD 15 [3]

Parameter	Value
Mass	3400 g
Power	6.5 W
Size	206x206x168 mm
Data Interface	1553 data protocol
Accuracy	0.035° or 126 arcsecond (3 σ)
Reliability	<1095 FIT @30 °C

Star sensor

Star sensors use stars and constellations in the sky to determine the current attitude of the spacecraft. They can be very accurate, however that makes the sensors a bit more complex, resulting in greater power consumption, size and mass. Different levels of performance of star sensors also exist. Here the specifications for four different star sensors are shown in Table 2.4 and Table 2.5. As examples the larger Jena Optronik ASTRO APS [4] and the Vectronic Aerospace VST-68M [5] are shown in Figure 2.4 and Figure 2.5.

2. SUBSYSTEMS DETAIL DESIGN

Table 2.4: Specifications of ASTRO 15 and VST-68M [6] [5]

Specifications	ASTRO 15	VST-68M
Mass	4500 g	470 g
Size	192 mm Ø x 552 mm	60x60x138 mm
Power	<10 W without cooling, <15 W with cooling	<3 W
Data Interface	RS422 or MIL-STD-1553B	2x RS422 or 2x CAN
Accuracy	<1 arcsec (1σ) for x,y, <10 arcsec (1σ) for z	<5 arcsec (2σ) for x,y, <30 arcsec (2σ) for z
Max slew rate	<0.3 °/s, reduced performance: 0.3-2 °/s	<3 °/s
Reliability	not available "design for 25 years GEO environment"	not available

Table 2.5: Specifications of ASTRO APS and VST-41M [4] [5]

Specifications	ASTRO APS	VST-41M
Mass	2000 g	900 g
Size	154 x 154 x 237 mm	80x100x180 mm
Power	<6 W without cooling, <12 W with cooling	<2.5 W
Data Interface	RS422 or MIL-STD-1553B	RS422 or RS485
Accuracy	<1 arcsec (1σ) for x,y, <8 arcsec (1σ) for z	<18 arcsec (2σ) for x,y, <122 arcsec (2σ) for z
Max slew rate	<0.3 °/s, reduced performance: 0.3-2 °/s	<3 °/s
Reliability	460 FIT@ 20°C	not available



Figure 2.4: Jena Optronik ASTRO APS



Figure 2.5: Vectronic Aerospace VST-41M

Gyroscope

The gyroscopes of a spacecraft are important for fast attitude determination. They have a high short-term accuracy [7], but they generally have a relatively high chance of failure, especially in long missions. In table 2.6 the ASTRIX 1120 and the CIRUS-EX are compared.

Table 2.6: Specifications of ASTRIX 1120 [8] and CIRUS-EX [9]

Specifications	ASTRIX 1120	CIRUS-EX
Mass	4.5 kg	16.8 kg
Size	263 mm Ø x h 192 mm	364.5x364.5x222.3 mm
Power	13.5 W	40 W
Stability	<0.003°/hr	0.0003°/hr
Angle random walk	< 0.002° / $\sqrt{\text{hr}}$	0.000125° / $\sqrt{\text{hr}}$
Reliability	"More than 15 years continuous operation"	0.93 for 15 year long mission (at 30°C)

As can be seen in table 2.6, the ASTRIX gyroscope is considerably lighter than CIRUS-EX. However, the ASTRIX is only redundant when it is combined with a second one [8]. The CIRUS already has redundancy on its own due to using four single gyroscopes. Even two ASTRIX gyroscopes are lighter than one CIRUS-EX gyroscope. However, the CIRUS-EX gyroscope is around an order of magnitude more stable and random walk also is substantially less, than for the ASTRIX 1120. The gyroscopes are shown in Figure 2.6 and Figure 2.7.



Figure 2.6: ASTRIX 1120



Figure 2.7: CIRUS-EX

2.1.2 ADCS Actuators

Once the attitude is known, maneuvers might be required in order to get the spacecraft positioned correctly. This is needed in order to point the devices such as the payload, antenna or solar panels in the right direction. This is done using actuators, multiple different types of actuators are discussed in this subsection. The use of RCS thrusters, reaction wheels, control moment gyroscopes and magnetorquers is discussed.

RCS Thrusters

Thrusters expel some propellant to generate a force on the spacecraft. For ADCS applications these are placed on opposite sides such that they produce two opposing force vectors, which do not point through the center of mass. This produces a torque without translating the spacecraft. Thrusters provide a way of external momentum exchange, thus only being limited by the propellant available.

The aerospace company Aerojet Rocketdyne is a well-respected aerospace company specialized in energetics systems and propulsion. For example, Aerojet Rocketdyne has continued working on the R-4D RCS thrusters, used in the Apollo Moon program. They have a broad range of RCS thrusters, of which two are especially attractive as they combine multiple nozzles pointing in different directions in one RCS module. This simplifies wiring as only a single module needs to be controlled. Moreover, both RCS thrusters use hydrazine as a propellant, which is the same as was decided in Work Package 2.

In Table 2.7 three different thrusters are compared, with the major difference between them being the thrust level and packaging. The Aerojet Rocketdyne MRM 106F and MRM 122 are both three clustered thrusters with the major difference being the different thrust levels of 40 N and 51-142 N respectively. The MONARC-5 is a single thruster with an even lower thrust level of just 4.5 N.

2. SUBSYSTEMS DETAIL DESIGN

Table 2.7: Specifications of RCS thrusters [aerojetrocketdyne2020 \cite {moog2018}]

Specifications	<i>MRM – 106F</i>	<i>MRM – 122</i>	<i>MONARC – 5</i>
Total mass	< 2.23 kg	< 2.98 kg	0.49 kg
Dimensions (max.)	317 × 228 mm	285 × 275 mm	418 × 25 mm
Power	20.1 W nominal @ 28 Vdc & 21 °C	43 W max @ 32 Vdc & 4 °C	18 W
Thrust	40 N	142-51 N	4.5 N
Specific impulse	231 s	228-217 s	226.1 s
Total impulse	136,000 Ns	332,000 Ns	613,852 Ns
Total pulses	1,570	7,005	205,000
Steady state firing (cumulative)	2,991 s	2,684 s	-
Propellant	Hydrazine	Hydrazine	Hydrazine
Chamber Pressure	16 bar	2.0-5.4 bar	5.5-29.0 bar



Figure 2.8: MRM-106F [10] Figure 2.9: MRM-122 130N [10] Figure 2.10: MONARC-5 [11]

When comparing the RCS thrusters, it can be observed that the MONARC-5 is relatively light compared to the Aerojet Rocketdyne models, it uses less power and has a lot more total impulse compared to the other two. However, the MONARC-5 is the only RCS module that only thrusts in one direction, while the others have three nozzles per unit. This enables easier packaging. All three RCS thrusters use Hydrazine as their propellant. This is available from the main propellant tank already. With these differences in mind, the major difference between the three options are the thrust levels.

Reaction Wheels

Momentum or reaction wheels are a device for internal momentum exchange. Spinning up or down a small wheel inside the spacecraft will provide a torque on the spacecraft in the opposite direction, thus enabling precise control of the spacecraft's attitude. An advantage, compared to thrusters, is that reaction wheels only need power to operate, never running out of fuel. However, momentum can build up in the reaction wheels such that they no longer are able to accelerate to provide a torque. To remove this built up momentum an external momentum exchange device such as thrusters are required. Due to disturbance torques on the spacecraft this will be required every so often.

Table 2.8 lists the specifications of two examples for reaction wheels, the RSI 15-215/20 and RSI 45-75/60 made by Collins Aerospace [12].

Table 2.8: Information about two momentum wheels from Collins Aerospace[12]

Parameter	Value	
Component code	RSI 15-215/20	RSI 45-75/60
Angular momentum ¹ [Nm s]	15	45
Operational speed range [rpm]	± 2000	± 6000
Physical dimensions [mm ³]	310dia × 160	310dia × 160
Mass [kg]	7.7	7.7
Power consumption (steady state) ¹ [W]	15	22
Power consumption (maximum torque) ¹ [W]	90	90
Motor torque ¹ [mNm]	215	75
Thermal efficiency	-	-
Life time ² [years]	15	15

Note that the reliability of each reaction wheel could not be found and thus it was replaced by the life-time parameter. It is seen that the difference in maximum angular momentum comes from the maximum rotational speeds from both wheels. A picture of the RSI 45-75/60 reaction wheel is also provided in Figure 2.11.



Figure 2.11: Reaction/momentum wheel from Collins Aerospace

Control Moment Gyroscope

This kind of actuator consists of a momentum wheel with its rotational speed kept constant. By moving the rotational axis of this wheel a torque is produced as seen in Figure 2.12. Control Moment Gyroscopes (CMGs) usually have a very high rotation speed thus making a high torque possible. The drawback of this is that the components need to be manufactured to high tolerances and are expensive and heavy. Hence, they traditionally have been used on large spacecraft, a notable example being the International Space Station. Table 2.9 shows an example of such a CMG from AIRBUS, this model is adequate for satellites with a mass of 1000-2000 kg but was designed for a life time of ten years in LEO. It is assumed that the lifetime of the model can be assured for a mission around Jupiter, using protective material to account for radiations.

¹@ Nominal speed

²In orbit

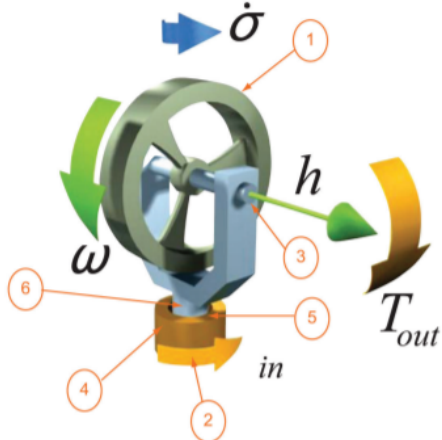


Figure 2.12: Representation of the control moment gyro [13]

As can be seen from Figure 2.12, this is a one gimble CMG, meaning that for complete attitude control, three are required, whereas for redundant operation four would be needed.

Magnetorquers

Magnetic torquers use the fact that a current flowing through a coil produces a magnetic field, which can interact with the magnetic field around it, thus producing a torque. Magnetic torquers can be used as a direct actuator of the ADCS or for momentum dumping for the reaction wheels. The torque generated is proportional to the number of coil turns, the area of each, the current that goes through them and the strength of the magnetic field at the position of the spacecraft[13]. Equations 2.1 and 2.2 describe the physics behind a magnetorquer.

$$D = N \cdot I \cdot A \quad (2.1)$$

$$\vec{M} = \vec{D} \times \vec{B} \quad (2.2)$$

Table 2.10 presents an example of magnetic torquer from Sinclair Interplanetary that could be used on-board of the JUICE mission. A picture of the same model is also provided in Figure 2.13.

Table 2.10: Example of a magnetorquer [15]



Figure 2.13: Magnetorquer example (QT-40)

Parameter	Value
Component code	TQ-40
Length [mm]	338 (single)
Mass [kg]	0.825 (single)
Resistance [Ω]	250 nominal per coil
Nominal dipole [Am^2]	42 @28V (3.136 W)
Maximum dipole [Am^2]	48 @34V (4.624 W)
Thermal efficiency	-
Life time ² [years]	-

Magnetorquers can only be used when there is a magnetic field around the spacecraft. Therefore, it could be used for momentum dumping on the JUICE mission once in orbit around Jupiter but they would be ineffective, while in the transfer orbit, as there is no magnetic field of sufficient strength. Note that the power consumed for a specific dipole can be found using $P = \frac{V^2}{R}$.

³Mechanism and electronics

⁴Quasi-static

⁵Max maneuver

2.2 Torque and Control Effects of the Actuators

In this section a detailed analysis and prediction of the torque and control effects of the actuators on the spacecraft will be presented. This is initially done by using the estimations from work package 2. Then those are refined by accounting for additional affects that could change how torque and control affects the spacecraft.

Operation modes and timeline

Before any calculations are made a brief review of the time line is given. The time line is given in Figure Figure 2.14. At different parts of the mission different ADCS modes are used. In the diagram the arrows with hollow heads give the most important ADCS modes used at that stage of the mission.

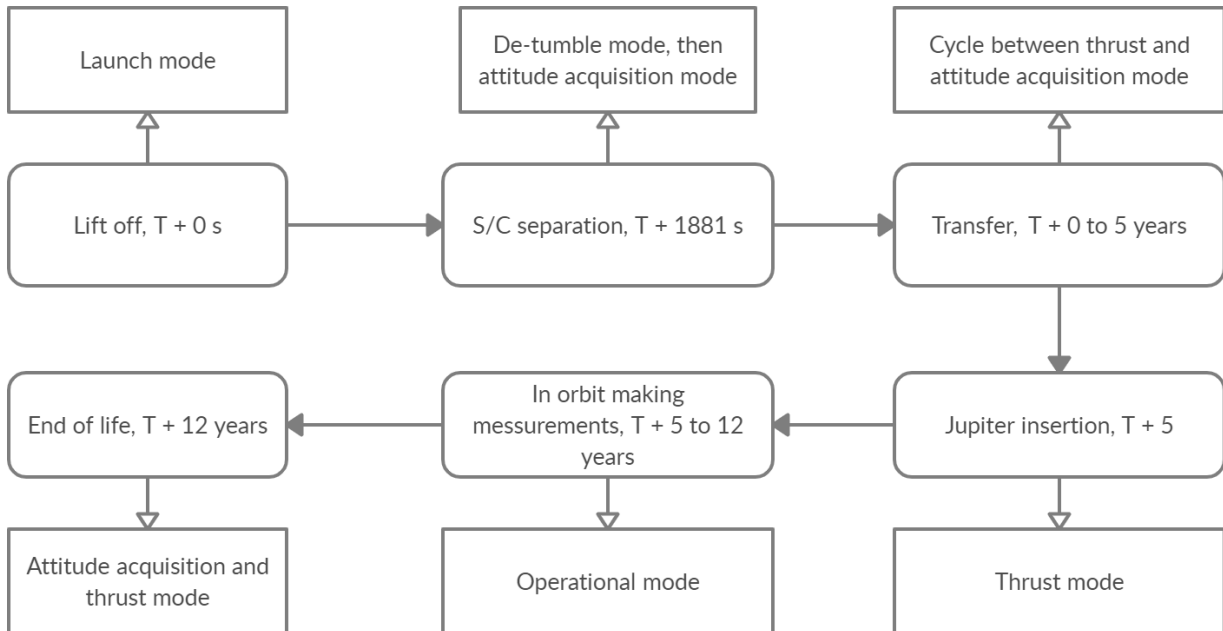


Figure 2.14: Timeline of the mission with important ADCS modes

At the start of the mission the launch mode is initiated. The ADCS system is put on idle and no control is directly performed on the spacecraft. This means that the launch vehicle performs all necessary actuations. The launch vehicle shall put the spacecraft into a heliocentric orbit before separation.

After separation the de-tumble mode is activated. Next to this communication mode will occasionally be turned on to communicate with the ground station, this holds for the entire mission. The de-tumble mode makes sure that the spacecraft keeps its attitude steady and that the rotations about the axis due to disturbance torques are close to zero. When the spacecraft is not rotating and the solar arrays are deployed the attitude acquisition mode is activated. In this mode the exact attitude is determined from multiple sensors and the gyroscopes are reset.

Then, the spacecraft is in transfer to Jupiter, and the thrust mode will be activated when a maneuver is required. The thrust mode ensures that the propulsion system is pointed correctly to get

⁶Note that in the diagram, Figure 2.14, an error has been made. The fourth part of the time line should indicate "Jupiter insertion, T + 5 years".

the most from the propellant used and the correct trajectory is attained. During the transfer the spacecraft will switch between attitude acquisition mode and thrust mode depending on the state of the spacecraft and whether the thrusters need to be fired. In this way the spacecraft can reset the gyroscopes and perform possible corrections to achieve the transfer.

Once Jupiter is reached, thrust mode is again initiated to perform the maneuver to a polar elliptical Sun synchronous orbit around the planet. In orbit the ADCS will activate operational mode. This mode makes sure that the payload instruments are pointed and stabilized as required by the mission phase. Finally, after twelve years the mission comes to an end. The spacecraft is put into thrust mode for a last time and the spacecraft will be de-orbited. This concludes the mission.

2.2.1 Structure Calculations

In this section calculations are made for the center of mass (COM), the center of pressure (COP) and the mass moments of inertia about the axis of the spacecraft.

Axis System

To make any calculations, an axis system has to be defined. The axis system is defined as shown in Figure 2.15.

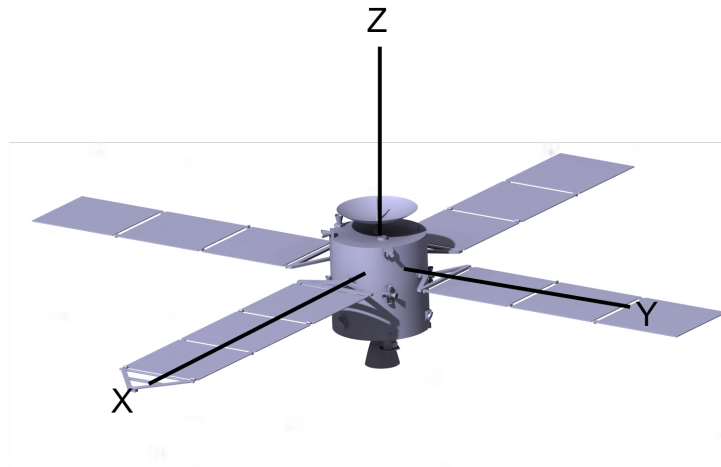


Figure 2.15: Axis system used

Spacecraft characteristics

To calculate the torques generated some more information of the spacecraft is required. Namely, the center of mass, the center of pressure and the moments of inertia of the spacecraft.

Center of Mass calculation

To determine the center of mass, it was assumed that the components act as point masses at their centroid. From workpackage 1 [16], the masses of the components are known. The position of the components are taken at the middle of the components. Due to symmetry, the COM for x-axis and y-axis will be calculated at the same time. However, first the COM for the z-axis is calculated. The bottom of the body is used as a reference point for distance when performing the COM calculations in the z-axis. The positions and masses were extracted from the CATIA model and can be found in Table 2.11. By taking the sum of the mass and the height mass product for all components and dividing the height mass product by the total mass the center of mass of the z-axis is found. It lies 1027 mm above the bottom of the body. In the calculation the ADCS, CDS, payload and thermal

subsystem are excluded. The position is not (easily) determined and their masses are negligible. Note that the total mass therefore is only valid for the center of mass calculation, the real total mass of the spacecraft is 2304.2 kg.

Table 2.11: Center of mass calculations z axis

S/C component	Height [mm]	Mass [kg]	Height x Mass
Communications	3400	72.0	244732
EPS	1900	409.2	777457.2
Harness	1500	91.6	137433
Structure and mechanisms	1900	178.5	339123.4
Propellant	475	1116.8	530494.25
Propulsion system	475	202.2	96023.15
Total	1027	2070.3	2125263

For the deployed and undeployed state of the spacecraft this figure 2.16 represents the estimated mass distribution of the system. As portrayed by 2.16, only the positions of the heavy masses (propellant+propellant tank mass) that have a center of mass outside the center of pressure are taken into account in the calculations, however the rest of the mass is assumed to lie on the center of pressure.

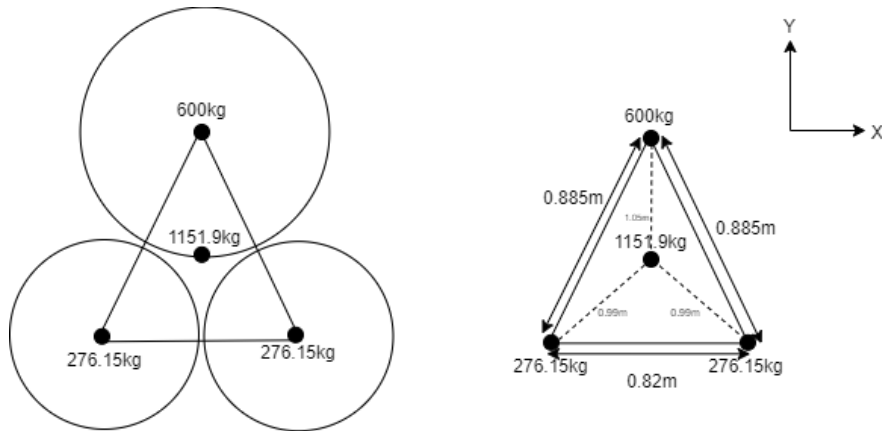


Figure 2.16: Center of Mass

It is apparent from 2.16 that the center of mass in the x-axis will lie on the symmetry axis of the triangle (an imaginary line connecting the bottom of the triangle, the 600kg point mass and the 1151.9kg point mass), however to get the center of mass on the y-axis the calculation is preformed in 2.3 :

$$Y_{com} = \frac{\Sigma M \cdot y}{M} = \frac{600 \cdot 1.05 - 0.901 \cdot 552.3}{2304.2} = 0.0575m \quad (2.3)$$

According to 2.3, the center of mass lies 0.0575 m away from the center of pressure (center of pressure lies on the axis of symmetry of the primary cylinder structure).

Center of Pressure Calculations

The center of pressure calculations were done only based on the surface area of the sketches and no mass has to be taken into account. To calculate the center of pressure Equation 2.4 can be used [7]:

$$CP = \frac{\sum A \cdot d}{\sum A} \quad (2.4)$$

Where A is the area of the section taken into account and d is the distance of the center of that section to the reference point.

Two different Cp positions need to be distinguished, one for the z-axis of the spacecraft and one for the y/x-axis. In the x/y-axis, the solar panels are mounted opposite to each other and have equal areas, therefore the center of pressure lies in the middle of the spacecraft, at the symmetry point.

For the z-axis, the spacecraft can be approximated by three simple shapes: a triangle for the engine, a square for the body and a semicircle for the antenna. This is shown in Figure 2.17, where the dimensions of each measurement are in meters. The CP lies on the z-axis of the spacecraft since it is symmetrical with respect to that axis, however the height of CP still needs to be determined. Using this approximations Equation 2.4 can be rewritten as Equation 2.5 in order to calculate z :

$$CP = \frac{9(0.54 + 1.5) + 0.078 \cdot 2/3 \cdot 0.54 + 2.454(0.720 + 3 + 0.54)}{9 + 2.454 + 0.078} = 2.51m \quad (2.5)$$

So, the center of pressure lies 2.51m from the bottom of the main engine, as showed in Figure 2.17

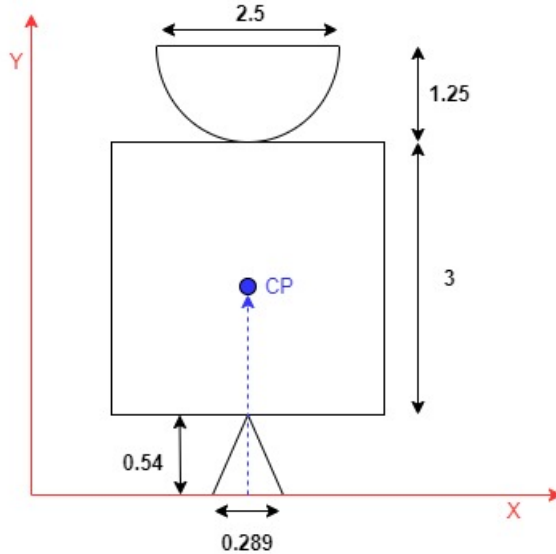


Figure 2.17: Dimensions for center of pressure in [m]

Moment Of inertia Calculations

As was already explained in the previous sections, the spacecraft is symmetrical with respect to the longitudinal axis z , therefore the moments of inertia about the y and x axis is going to be the same. The moments of inertia are calculated below, taking into account the mass of the spacecraft's different parts where $m_{sc} = 1993.7kg$ and $m_{panels} = 313.2kg$:

Assumptions

- The center of mass with respect to the z -axis is considered negligible in the calculations, since the number is not very significant. Therefore, for I_z the center of mass is considered to lie on the center of pressure
- Masses of the solar panels and the rest of the spacecraft is used in the calculations as point masses for simplicity

$$I_x = I_y = \frac{1}{12}m_{sc}(3 \cdot 1.5^2 + 3^2) + m_{sc}(0.4^2) + \frac{1}{12}m_{panels}(9^2 + 2.75^2) + \frac{1}{2}m_{panels}(6^2) + m_{panels}(0.8^2) \quad (2.6)$$

$$I_x = I_y = 11084.22kgm^2 \quad (2.7)$$

$$I_z = \frac{1}{12}m_{sc}(1.5^2) + \frac{1}{2}m_{panels}6^2 + \frac{1}{12}m_{panels}(2.75^2 + 9^2) = 8322.8kgm^2 \quad (2.8)$$

2.2.2 Disturbance Torques

In this subsection the different types of torques are described.

Gravity Gradient

The gravity gradient torque [17] occurs, when different parts of the spacecraft experience different gravitational accelerations, therefore they move at different rates causing torque to be induced. The torque is given by Equation 2.9:

$$T_g = \left(\frac{3\mu}{2R^3} \right) [I_z - I_y] \cdot \sin(2\theta) \quad (2.9)$$

Solar radiation pressure

Solar radiation pressure [17] is caused by photons striking the surface of the spacecraft causing it to have a torque, the force that causes this torque is represented by Equation 2.10:

$$F_s = \left(\frac{F_s}{c} \cdot A_s \right) (1 + r) \cdot \cos(I) \quad (2.10)$$

$$T_s = F_s * r_p \quad (2.11)$$

however this force acts on the center of pressure of the spacecraft therefore to get the torque, the location of both the center of mass and the center of pressure is essential for this calculation. 2.11 Could be used to transform the force caused by the solar radiation pressure F_s into Torque, this is done by multiplying the force by the distance between the center of pressure and the center of mass r_p in the respective axis, where the photons strike the surface of the spacecraft.

Magnetic Torque

As charged particles impact the surface of the spacecraft, the spacecraft will induce a positive/negative charge, this charge will be the main factor that causes the magnetic torque 2.12 on the spacecraft, since the spacecraft's magnetic field has to align with the magnetic field of planet orbited. this torque is represented by Equation 2.12:

$$\vec{T}_m = \vec{B} \times \vec{D} \quad (2.12)$$

Aerodynamic Drag

As a result of different components of the spacecraft having different Drag coefficients, the spacecraft experiences Drag torque, however since there are multiple forces in different directions torques occur in many axis's therefore the formula for the drag force is given by Equation 2.13:

$$F_d = \frac{1}{2}C_d\rho V^2 A \quad (2.13)$$

However at very high altitudes and on Jupiter the atmospheric density ρ is very small therefore this force can be considered negligible

Internally generated torques

During orbit, the spacecraft can experience internal disturbance torques, due to intentional or accidental mass expulsion or due to operating machinery, such as motion of solar arrays, antennas or deployment of booms and appendages. Equation 2.14 gives the internal generated torque as a function of the force and the moment arm

$$\vec{T} = \vec{F} \times \vec{r} \quad (2.14)$$

Where F is the disturbance force that acts on the spacecraft body and r is the distance to the center of mass.

2.2.3 Actuator Torque and control effects

Analysis of mission timeline

In this section the different mission timelines are covered in greater detail. Specifically, the disturbance torques they counteract in different phases of the mission.

Firstly, the spacecraft will be analysed when it is separated from the launch vehicle and its in heliocentric orbit. A great advantage of being in heliocentric orbit is that the gravity gradient, Magnetic Torque and Aerodynamic Drag are negligible since the spacecraft is no longer nearby a celestial body, therefore only the solar radiation pressure is taken into account as a disturbance torque. given that in our calculations the worst case scenario will be taken into account, the surface area would be 105.6 (solar arrays+ 1 surface of the primary structure), the incidence angle taken is considered to be zero and for the surface reflection of the surface, $r=1$.[17] $F_s = 1358W/m^2$

$$F = \left(\frac{F_s}{c} \cdot A_s \right) (1 + r) \cdot \cos(I) = \left(\frac{1358}{3 \cdot 10^8} 105.57 \right) (1 + 1) \cdot \cos(0) = 9.558 \cdot 10^{-4} N \quad (2.15)$$

this total force, caused by the solar radiation pressure, on the Z axis is $9.558 \cdot 10^{-4} N$ and since the difference between the center of pressure and center of mass is 0.0575, thus the torque is $5.5 \cdot 10^{-5} Nm$ however for the X or Y axis the force becomes as follows:[17]

$$F = \left(\frac{F_s}{c} \cdot A_s \right) (1 + r) \cdot \cos(I) = \left(\frac{1358}{3 \cdot 10^8} 4.5 \right) (2) \cos(0) = 4.074 \cdot 10^{-5} N \quad (2.16)$$

and consequently this force of $4.074 \cdot 10^{-5} N$ lies a distance of 0.87 m away from the center of mass in the X or Y axis, which causes a torque of $3.54 \cdot 10^{-5} N$.

As the mission proceeds the solar radiation pressure is reduced, since the spacecraft is moving away from the sun. Moreover, once the spacecraft begins the propulsion system to move towards the intended destination, fuel sloshing starts to take place,[18] fuel sloshing occurs as a result of the fuels movement inside the spacecraft. However, since the sloshing effects are very computationally intensive and out of the scope of this course the disturbance torque caused by this factor is ignored and instead recommendations to the spacecraft will be presented in order to reduce the effects of sloshing.

Furthermore, once the spacecraft reaches Jupiter, the spacecraft will experience Magnetic Torque and Gravity Gradient Torque. Other torques like solar radiation pressure and aerodynamic drag are ignored, since the forces produced are negligible/non-existent.

For the Gravity Gradient an angle θ of 45 degrees is used, in order to account for the maximum gravity gradient during the orbit of Jupiter 2.17 will be used: [17]

$$T_g = \left(\frac{3\mu}{2R^3} \right) [I_z - I_y] \cdot \sin(2\theta) = \frac{1.26686535 \cdot 10^{17}}{2 \cdot 78492000^3} (2761.42) \sin(90) = 3.62 \cdot 10^{-4} Nm \quad (2.17)$$

and for the magnetic torque a value of 1 is used for c and a value of $2.83 \cdot 10^{20} T \cdot m^3$ is used for the magnetic moment of Jupiter μ_j and consequently this formula is used:[17]

$$\vec{T}_m = \vec{B} \times \vec{D} = \frac{\mu_j}{cR^3} = 5.85 \cdot 10^{-4} Nm \quad (2.18)$$

in addition to the torque effects during the Jupiter orbit, the spacecraft will also experience orbital perturbations [19]

$$\mathbf{a}_p = \mu_p \left(\frac{\mathbf{r}_{ps}}{\|\mathbf{r}_{ps}\|^3} - \frac{\mathbf{r}_p}{\|\mathbf{r}_p\|^3} \right) \quad (2.19)$$

Equation 2.19 will be used to find the acceleration that the spacecraft experiences due to the Jupiter moons, however for the spacecraft it is assumed that only two moons (Io and Europa) affect its orbit, this is because these moons have a distance much closer to Jupiter than other bodies. For the simplicity of the equations and to get the maximum orbital perturbation it is assumed that Jupiter and the two moons with the spacecraft between them lie on one line. the distance between the spacecraft and perturbing body is given by r_{ps} whilst the distance between the orbiting body and the perturbing body is given by r_p . the gravitational constant of the perturbing body is given by μ_p .

First, the acceleration caused by the Moon Io is taken into account:

$$a_{p1} = 5.96 \cdot 10^{12} \{(5.8 \cdot 10^{-18}) - (5.62 \cdot 10^{-18})\} = 1.0728 \cdot 10^{-6} ms^{-2} \quad (2.20)$$

and for the Europa Moon the result is as follows:

$$a_{p2} = 2.27 \cdot 10^{12} \{(2.27 \cdot 10^{-18}) - (2.22 \cdot 10^{-18})\} = 1.6 \cdot 10^{-7} ms^{-2} \quad (2.21)$$

the addition of both of these accelerations influenced by the moons of Jupiter causes a total acceleration of $1.2328 \cdot 10^{-6} ms^{-2}$

Momentum wheel and thruster effects

Table 2.12 presents the different torques caused by different external disturbance forces during various points in the mission.

Table 2.12: Disturbance torques

Mission Timeline	Value of Torque
Heliocentric Orbit	$9.558 \cdot 10^{-4} Nm$
Maneuvering	-
Jupiter Orbit	$9.45 \cdot 10^{-4} Nm$

Reaction Wheel

According to the table 2.12, the highest possible torque occurs when the spacecraft is in heliocentric orbit, since it has a torque of $9.558 \cdot 10^{-4} Nm$, during the orbit around Jupiter the reaction wheels should be able to counteract this torque. Using a margin factor of 2 [13], the torque to be provided by the momentum wheel is estimated to be $T_{RW} = T_D \cdot (1 + MF) = 2.867 mNm$. For attitude adjustments the maximum torque is dependent on the reaction wheel used, as described in subsubsection 2.1.2.

Thrusters

Since the reaction wheels have a maximum angular momentum storage of 15 Nms, once the reaction wheels reach that point it should dump its momentum, in order to continue producing the required torque. The thrusters will produce the required torque that will dump the momentum the reaction

wheels have built up. It is assumed that the momentum dumping will utilize 2 thrusters of 40 N described earlier in subsubsection 2.1.2. They are placed at the outer edges of the spacecraft to have a moment arm of 1.5 m in the intended direction. The resulting maximum torque during momentum dumping is calculated in Equation 2.22

$$T = 2F_t \cdot L_m = 120Nm \quad (2.22)$$

2.2.4 Recommendations

To optimize the design, recommendations are made for the torques and other effects. This will be done for the disturbance torques and for the sloshing of the fuel.

Optimisation for external disturbances

- **Gravity gradient:** To minimize the torque caused by the gravity gradient, the mass of the spacecraft should be distributed as much as possible along the direction of the gravity field.
- **Solar radiation pressure:** The solar radiation pressure is kept minimal, when the absorbing area is minimal and when the center of pressure and mass align. Minimizing the absorbing area is not always possible due to other constraints, however aligning the COM with the COP is feasible.

Optimisation for internal disturbances

Next to the external disturbances are internal disturbances. When the thrusters stop accelerating the spacecraft, the fuel is not accelerated anymore and small accelerations can cause it to move around, or "slosh". The movement of the propellant can cause control issues. This effect should definitely be kept to a minimum. To limit the amount of sloshing:

- Tanks can be divided with baffles and bladders;
- Fuel can be allowed to settle after a manoeuvre;
- The change in angular velocity can be lowered to avoid fluid excitation;
- Notch filters can be installed.

However, each solution comes with a cost. Baffles and bladders add weight, which in turn add extra costs. Allowing the fuel to settle causes the mission availability to decrease. Smoothing the change in angular velocity of the spacecraft limits the agility of the spacecraft. And finally, adding notch filters reduces the spacecraft control bandwidth. Notch filters are designed to remove a band of interference, however this also limits the control capabilities of the spacecraft. In addition to that, to increase the effectiveness of the thrusters, it is recommended to increase the moment arm in order to increase the torque produced and thus decrease the propellant used for the thrusters.

2.3 Possible Configurations of the Subsystem

This section proposes multiple possible configurations for both the sensors and actuators that can be used to determine and control the attitude. There are multiple things to consider such as accuracy, reliability and redundancy.

2.3.1 Sensor configurations

From the previously explored sensors there are not too many possible combinations. The major choices thus far are the number and placement of the sensors. Some of the choices will be explained here.

- **S1 (Figure A.1): One star sensor and three gyroscopes.** This configuration is the one with the fewest sensors, it can provide an accurate attitude from the high accuracy star sensor ASTRO APS and further inertial measurements using ASTRIX 1120 gyros. In case of tumbling, however the star sensor cannot determine an accurate reading for de-tumbling, thus not being able to control the spacecraft anymore. In case of failure of one sensor component there will be no backup, so the ADCS is severely harmed and can most likely not determine an attitude accurately anymore.
- **S2 (Figure A.3): Three coarse sun sensors, two star sensors and six gyroscopes.** This configuration uses two star sensors, one high accuracy ASTRO APS and one lighter, lower accuracy VST-41M, mounted on the outside of the spacecraft, pointing in orthogonal directions. Therefore, a higher accuracy can be achieved due to higher star sensor accuracy in the xy plane of each sensor. This also ensures in case of failure of one star sensor that the other one can still be used for high accuracy attitude determination. In case of higher angular velocities the sun sensors can provide a less accurate reading for de-tumbling. They are arranged in 3 different axis so the sun will be visible, when rotating around any axis. The two units of ASTRIX 1120 gyros also provide redundancy, and is chosen due to their lower weight and power with two units than the other option which is inherently redundant. Hence, this configuration is very failure resistant.
- **S3 (Figure A.2): One fine sun sensor, one horizon sensor, one star sensor and six gyroscopes.** The star sensor ASTRO APS is the highest accuracy sensor on-board, which can give full three axis pointing information during all mission phases. Inertial pointing knowledge is provided by two redundant ASTRIX 1120 gyroscopes. For higher slew rates the fine sun sensor can give readings to de-tumble. In case of failure of one component the remaining sensors can still provide a fairly precise full three axis reading provided the failure does not occur on the star sensor, while not in the vicinity of a planet where the horizon sensor works.
- **S4 (Figure A.4): Three star sensors, eight coarse sun sensors, six gyroscopes.** The star sensors are currently the most common ADCS determination device and will be used on-board of the JUICE mission as well. For an accurate reading, the two vectors required for attitude determination should be placed at a large angle, thus two high accuracy ASTRO 15 star sensors are used at the same time as the main way to determine the attitude. A third one is added to avoid single point of failures, the lower accuracy VST-68M is used as it is a lot less heavy. Unfortunately, star sensors cannot be used in case the rotational speed of the spacecraft is larger than $2^\circ/\text{s}$ as seen from section 2.1 (and their accuracy decreases greatly if larger than $0.3^\circ/\text{s}$). Therefore, Bradford CSS eight coarse sun sensors should also be part of the configuration to enable attitude determination just after the separation of the launch vehicle or the kick stage as tumbling will occur. In practice, only two sensors are required for attitude determination, but it is important to make that at least two of those have the Sun in view for any tumbling mode. Therefore, two on each end of the solar panels are used for redundancy, their field of view being 180° , it is guaranteed that the Sun is in the range of at least two of them. Lastly, four lower accuracy ASTRIX 1120 gyroscopes are used for relative attitude determination, those are important in case of maneuvers as star sensors are rather slow to make measurements and gyros can get quick results, if they have a known value of the attitude of the spacecraft before the maneuver. Four of them are used as three are necessary for attitude determination and the last one is added for redundancy.

Details about the sensors can be found in section 2.1.

2.3.2 Actuator configurations

Several different configurations can be formed using the actuators described in section 2.1, this will be done based on several points of importance. First, there should be no singular points of failure, which means that in the case that one actuator fails, the ADCS should still be able to function properly. This is ensured by the redundancy of the system. Then, the spacecraft is designed for three axis stabilisation, meaning that there must be at least one actuator on each axis.

- **A1 (Figure A.1): Four momentum wheels and four RCS thrusters.** The RSI 15-215/20 momentum wheels permit to perform all ADCS maneuvers in an accurate manner and to provide gyroscopic stiffness. The main downside is that they will store angular momentum during operations and dumping will be required. Therefore, thrusters are needed in addition to the wheel for dumping of the angular momentum stored, this is typically done once per orbit. Having four momentum wheels in a pyramid configuration avoids any singular point of failure related to those as in case one fails, three reaction wheels are still operational. Four MRM-106F thrusters are necessary for momentum dumping, as each is composed of three nozzles (one in each axis). No redundancy is added as thrusters are simple devices and usually have a high reliability⁶ (represented by the large total impulse and total number of pulses)
- **A2 (Figure A.2): Four CMGs, twenty-four thrusters.** A configuration that makes use of four control moment gyroscopes allow for more torque generation with less energy required than using reaction wheels. The use of CMG 40-60S however, requires a more sophisticated steering algorithm than using momentum wheels as the change in torque and angular momentum needs to be taken into account. Even if only three CMGs are required to perform all maneuvers, a fourth one is added for redundancy. In addition to the CMGs, twenty-four MONARC-5 thrusters are required for dumping the stored angular momentum. As explained in configuration A1, a pair of thrusters is placed in each direction for each axis. This ensures redundancy and three-axis full control.
- **A3 (Figure A.4): Four momentum wheels, twelve thrusters and three magnetorquers.** The four momentum wheels used would be the RSI 15-215/20 and the thrusters would be the MONARC-5 ones since they offer the possibility of having the pairs separated. The redundancy is ensured by the QT-40 magnetorquers, in order to reduce the total weight of the ADCS. The main issue arising then is linked to the fact that magnetorquers need to be in a strong magnetosphere to be effective and thus those would not be effective during the transfer orbit.

⁷Note that even the Apollo 11 mission to the Moon had only twelve thrusters (no redundancy)[20]

Baseline Selection 3

In this chapter the previously created configurations will be analyzed and a trade off will be created. First, criteria for the trade off will be defined and given weights. Each configuration will then be assigned a score, of which the configuration with the highest score will be selected for the design.

3.1 Trade Off Criteria

For a trade off to be done, there need to be multiple criteria that are evaluated for each option. Each of these criteria are then given a weight based on the importance of that criteria. The scores of all configurations are then multiplied by the weight and added up to form a final score. The option with the highest score is the winner and is then chosen.

For this assignment we will chose the following criteria:

- Reliability, weight: 30%. The Reliability of the sensors and actuators are paramount to the mission succeeding. It gives the probability that no component fails. As the ACDS is a system that is often the cause of failures that end missions prematurely and considering the lengthy mission with a high reliability requirement, this criteria has been given a large weight of 30%.
- Power, weight: 10%. Most sensors consume some amount of power to determine the attitude. Since the spacecraft will be far away from the Sun and use solar power, any additional power consumption will increase the size of that system. Thus, low power consumption is desirable. For actuators both the peak and average power consumption will be listed, upon which the scores will be assigned.
- Mass, weight: 10% The mass is as on all spacecraft a criteria that needs to be considered as every additional mass has a great penalty. Increasing mass increases the propellant mass needed to provide the required propulsion. This further requires design changes that increase mass, known as the snowball effect. For this mission however, the preliminary budgets have a large margin and even at the maximum of those margins the launch vehicle is still more than capable to launch the spacecraft to its required trajectory. Thus mass is only weighted with 10% in this trade off, as other factors, especially the reliability are favored.
- Accuracy 20% The ADCS is of course responsible for pointing the spacecraft in the required directions. Thus both the sensors need to be able to determine the current attitude to some degree of precision. Conversely the actuators have to be able to create torques precisely, and have sufficient amounts of torque actuate the spacecraft at the required rates. This criteria receives a weight of 20% since the pointing requirements of this spacecraft as defined in WP2 are not the most stringent compared to many other similar spacecraft.
- Redundancy 30% If the system is designed redundantly and a component fails, a redundant system will continue working with a backup at either the same level or with degraded performance. Thus integrating redundancies in the system will raise the probability that the mission succeeds,

3. BASELINE SELECTION

or can at least partially achieve its targets. Similar to the reliability, this criteria has a high weight of 30% as it is closely coupled to the probability of achieving the mission.

This trade off will be performed separately for the sensors and actuators, as they perform their task independently and can thus be selected, without much consideration of the other parts of the ADCS. Each configuration will be evaluated based on the previously criteria by assigning a score between one and five to each criteria. Each score is multiplied by its weight, thus arriving at a final weighted score. The configuration achieving the best weighted score will be selected.

3.2 Trade Off

3.2.1 Sensor Configuration Trade Off

Table 3.1 provides the trade off performed for the sensor configurations. According to that, the configuration S2 using three coarse sun sensors, two star sensors and six gyroscopes is suited best for this mission.

Table 3.1: Trade off table for sensor configuration

Criteria	Reliability(30%)	Power(10%)	Mass(10%)	Accuracy(20%)	Redundancy(30%)	Weighted Total
S1	4	5 (25.5 W)	5 (6.5 kg)	4	1	3.3
S2	4	3 (42 W)	3 (14.615 kg)	5	4	4
S3	2	3 (45.75 W)	3 (14.775 kg)	4	2	2.6
S4	4	1 (60 W)	1 (20.19 kg)	5	5	3.9

The values for reliability for each configuration are very similar, as each configuration uses the same components with the same reliabilities, apart from S2, which has a horizon sensor and fine sun sensor with worse reliabilities compared to the other systems. For the power and mass rankings, the values of each configurations were computed, upon which the scores are based. Accuracy is very similar across the board, with S2 and S4 scoring higher due to having multiple star sensors which allows for superimposing the measurements. The redundancy score is based on how many components can fail and at which mission phases without compromising the attitude sensing abilities. It was thus decided to use the S2 configuration.

3.2.2 Actuator Configuration Trade Off

The different actuator configurations will be traded off in a similar manner to the sensors. The results of this can be seen in table Table 3.2, showing that the configuration A1, using 4 reaction wheels as well as 4 thruster assemblies each with 3 nozzles, is the winner.

Table 3.2: Trade off table for actuator configuration

Criteria	Reliability(30%)	Power(10%)	Mass(10%)	Accuracy(20%)	Redundancy(30%)	Weighted Total
A1	4	4 (440.4/60 W)	4 (39.72 kg)	4	4	4.0
A2	3	1 (892/220 W)	1 (163.76 kg)	5	4	3.2
A3	3	3 (590/60 W)	4 (39.155 kg)	4	5	3.9

The scores for the criteria reliability are similar, due to the small difference between CMGs and reaction wheels. However, as CMGs are relatively novel for applications on smaller spacecraft, they were ranked lower than traditional reaction wheels. A3 received a penalty in reliability as the magnetorquers are not always available. Power and mass was scored similarly to the sensors, calculating the exact values and basing the scores on the values. For the actuators the accuracy also took into account the amount of torque available to rotate the spacecraft. Therefore, the CMG

configuration scored highest. Redundancy was scored based on what components can fail without endangering the completion of the mission. All configurations scored highly, however the configuration using both magnetorquers and thrusters excelled on this criteria, as this provides two independent ways to dump momentum, with each being redundantly built. It was thus decided to use the A1 configuration.

3.3 CATIA Kinematic Model

Now the configuration of the sensors and actuators is known, the architecture of the spacecraft can be updated and a kinematic model of the spacecraft using its actuators can be made. First the updated architecture will be showed and then the kinematic model will be generated.

3.3.1 Updated Spacecraft Architecture

As mentioned in Work-package 2 [21], the payload was placed close to the engines, which could cause problems. Now a solution is found, which is to change the orientation of the spacecraft such that its side faces Jupiter. Now the payload can be placed on top where no thrusters are mounted (Fig. 3.1) and they can still observe the planet. Furthermore, the solar panels can now orientate to the sun more easily in the designed orbit, which is sun-synchronous, polar and orientated such that there is no eclipse. Also, instead of the reaction wheels to be placed at the outsides of the spcecraft, a tetrahedon with the four wheels placed on top is placed inside the bus (Fig.3.3).

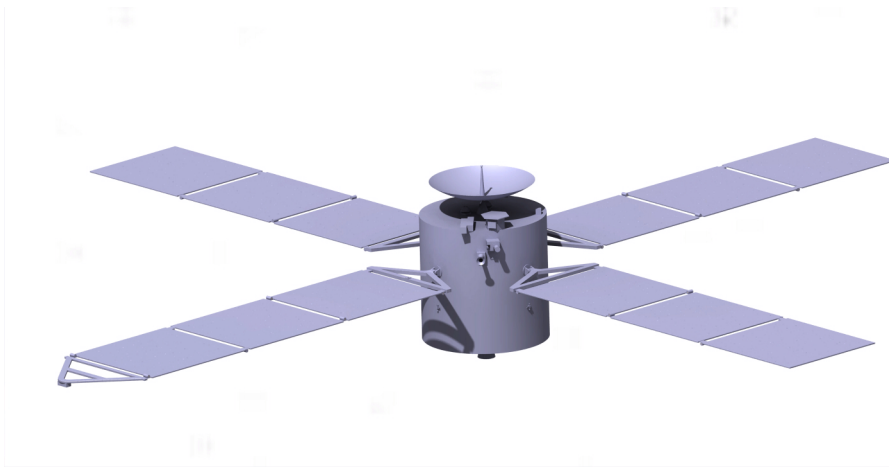


Figure 3.1: The Side of JUICE facing Jupiter

3.3.2 Kinematic Models

In Section 3.2 it was found that configuration S2 with A1 is the best. So the four momentum wheels will be the primary actuators for the attitude control. By varying their spinning directions and speeds, it is possible to let the spacecraft rotate in any desired direction. In the following simulations of which the initial positions are given in Fig. 3.2 and Fig. 3.3 the spacecraft will be rotated 100 degrees around the z-axis (blue) and the x-axis (red). At the same time, the motions of the momentum wheels will be captured.

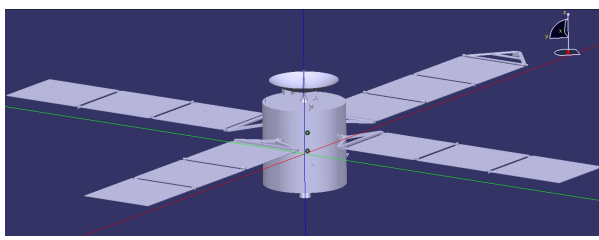


Figure 3.2: Initial view of the Spacecraft in model

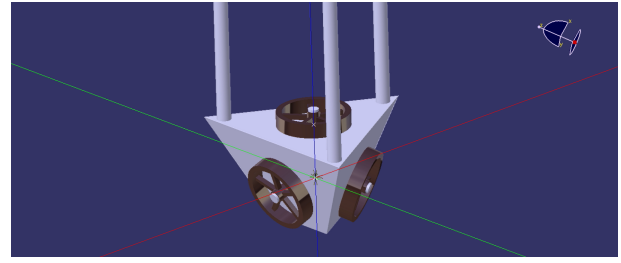


Figure 3.3: Initial View of the Momentum Wheels in model

Rotation around Z

For the spacecraft to rotate around the z-axis in the positive direction, the momentum wheels first need to generate a torque in the opposite direction to accelerate the spacecraft and then generate a torque in the direction of motion of the spacecraft to decelerate it, so the spacecraft comes to a stand still. For the momentum wheels to generate a net torque in the negative z-direction, the top wheel needs to accelerate clockwise and the other wheels need to accelerate counterclockwise. As can be seen in Fig. 3.4 the x and y components of the torques generated by the side wheels will cancel if these accelerate at the same rate. So the net torque will be in the negative z-direction. In order to stop the spacecraft at the end of the manoeuvre, half way through it, the wheels start decelerating at the same rate as they first accelerated causing an opposite torque to the spacecraft.

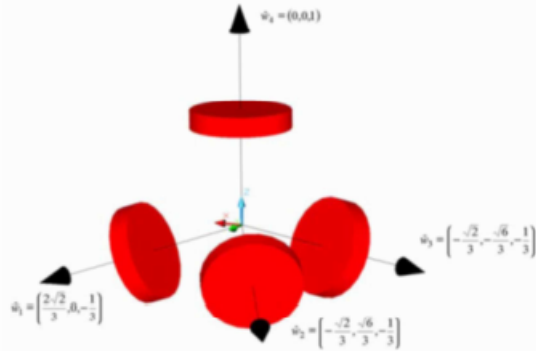


Figure 3.4: Pyramid Momentum Wheel Configuration [13]

Rotation around X

For the rotation around x, the same acceleration and deceleration will take place. However this time the reaction wheels spin differently. The side wheel intersecting the x-axis will accelerate clockwise and the other two wheels on the side will accelerate counterclockwise. As can be seen in Fig. 3.4, these two other side wheels will cancel each others torque in the y-direction, however, provided that the side wheels accelerate at the same rate, there is now still a torque in the negative z-direction, which is one third of the torque generated by one of the side wheels. To counteract that torque, the top wheel will accelerate counterclockwise at a third of the acceleration of the side wheels. The net effect is a torque on the spacecraft causing it to rotate around x positively.

Important Details

As can be noted, the spacecraft's attitude is changed in these simulations. However if the wheels are counteracting a disturbance torque, the process is slightly different. In that case they accelerate such that they generate an equal but opposite torque to the disturbance torque. If that disturbance torque is gone the wheels continue spinning at the same rate instead of decelerating like in the simulations. So

the spacecraft stays stable. Furthermore, the angular velocity of the reaction wheels in the simulations is reduced significantly in order to visualise the acceleration and deceleration of these. However, the acceleration of the spacecraft in the simulation is higher than it is in practice as its acceleration could not be made slower in CATIA. Lastly, it is not necessary for the wheels to start from a stand still, but it is clearer for the visualisation.

Subsystem Integration **4**

This chapter will give a detailed, but concise, description of the integration of the ADCS subsystem in the spacecraft. The design of the interface between the spacecraft and ADCS will be explained, using the chosen sensor and actuator configurations determined in section 3.2. Lastly, a detailed ADCS subsystem diagram will be provided, to demonstrate the integration of the ADCS subsystem with the spacecraft.

4.1 Integration of ADCS

In this part the mechanical integration of the ADCS, with all its components with the rest of the spacecraft, will be described.

4.1.1 Sensors

In order, to determine the attitude of the spacecraft, several sensors are used as stated before. These are three coarse sun sensors and two star sensors.

The three coarse sun sensors determine the attitude of the spacecraft, by comparing the spacecraft's attitude to the attitude of the Sun. Since these sensors are only used when the spacecraft is in a spin, at least three sensor are needed to detect the Sun's attitude in two directions. The three sensors should be placed on the three axes on the outside of the spacecraft. In this way, one of the sensors will always have the sun in its field of view when needed in a spin. The sensors are placed on the outside of the spacecraft and their field of view may not be obstructed by any other components.

Furthermore, the spacecraft is also equipped with two star sensors. Star sensors can determine the spacecraft's attitude by tracking and recognizing star constellations in the field of view, and comparing the view with saved star patterns. The star sensor should be placed on the outside of the spacecraft in such a way it has an unobstructed view on the stars without the sun near the field of view while operating. The star sensors are mounted orthogonal to each other, as the performance of star sensors is worse along the direction the lens is pointed. Thus mounting the sensors at 90 degrees to each other improves performance.

As is stated in determined in section 3.2, six gyroscopes will be used as well to determine the spacecraft's attitude without needing to continuously using the other sensors. No specific location within the spacecraft is required for them to operate. Three gyroscopes are combined within one unit as can be seen in figure 2.6. Since the second unit of gyroscopes is present for redundancy, it should be placed at another space within the spacecraft for safety reasons.

4.1.2 Actuators

As the trade off in section 3.2 has determined, the spacecraft will have four reaction wheels in order to control the spacecraft. To be efficient as possible the reaction wheels should be placed as close to the center of mass as possible. This is because, the reaction wheels can only rotate the spacecraft around its center of mass.

Furthermore, the spacecraft will have four RCS thrusters in addition to the reaction wheels for dumping angular momentum stored in the reaction wheels. RCS thrusters are capable of rotating the spacecraft due to the fact that a torque is generated when the thrusters are located off the center of mass. The torque generated is larger the larger the distance between the thruster and the center of mass. Conversely, an equal torque can be generated by a smaller thrust (i.e. consuming less fuel) when a thruster has a bigger momentum arm. Thereby, the thrusters should be able to rotate the spacecraft around the three axes. In order to do so, the four thrusters should be placed at four sides along the same axis. In conclusion, the RCS thrusters should be placed in such a way they have an optimum momentum arm, and they should be placed at four different sides along the same axis.

4.2 ADCS interface

As the final sensor and actuator configurations have been chosen, it is now important to design an interface between the ADCS subsystem and the spacecraft. The interface will consist of an electrical and data transmission interface from the sensors, which command to the actuator interfaces. It can be retrieved from Work Package 2 that the Galileo PDCU will be used, which is important as it has specific parameters. For example, the Galileo PDCU uses two Dual MIL-STD-1553, so the sensors and actuators ought to be able to connect.[22]

4.2.1 Electrical and Data Transmission Interface

Since, the sensor configuration consists of three coarse Sun sensors, two star sensors and six gyroscopes, it is of paramount importance to design a working interface between the sensors and the spacecraft. As for the coarse Sun sensors, the Bradford coarse Sun sensors were chosen, which is analog and uses four analog channels of 0-90 mV voltage mode for data transmission interface. While, in current mode will mode up to 35 mA and the power consumption is 0 W (passive CSS).

Moreover, the two star sensors are both different sensors, namely the ASTRO APS and the VST-68M. Firstly, the ASTRO APS uses the MIL-STD-1553B or RS 422 for the eletrical and data transmission interface, and the input voltage range is between 30-52 V DC and the power consumption is < 12W. As the PDCU consists of two Dual MIL-STD-1553, this will be chosen as the data interface for the ASTRO APS. Furthermore, the VST-68M uses two RS 422 standards for the data transmission interface, has a maximum power consumption of 3 W and an input voltage range (VDC) of 9-40 V. The connector used for the VST-68M is the MDM-25, which is able to connect the two RS 422 to the two Dual MIL-STD-1553.

The two ASTRIX 1120 gyroscope units chosen, consisting of six gyroscopes, use the MIL-STD-1553B technical standard for both, electrical and data transmission interface. The power budget per gyroscope unit is 13.5 W and it has an input voltage range of 22-50 V. Again, to simplify the electrical and data transmission interface interference, the same technical standard is used as for the Sun and star sensors, namely the MIL-STD-1553B.

4.2.2 Actuator interfaces

For the actuator configuration, it is chosen to go for four momentum wheels and four RCS thruster units, consisting of three thursters. Looking at the reaction wheels, it has been decided that the RSI

15-215/20 reaction wheels are the best option. This is mainly because of the ADCS maneuvers, which the spacecraft needs to perform.

The RSI 15-215/20 reaction wheels will use 15 to 90 watts of power each. The power consumption depends on the mode used. One reaction wheel needs 15 watts when in steady state and 90 watts when it is put to maximum torque mode [12]. However the maximum torque mode will rarely be used and the power can be provided by the PCDU, so no power problems are generated. It is not specified what interface these reaction wheels use, therefore it is assumed that they do not need any.

The specifications of the sensors and actuators are summarized in Table 4.1. In the Table some sensors and actuators are as a multiple, however the specification are given for a single unit.

Table 4.1: Types of sensors and actuators and their power consumption

Sensor or actuator	Power [W]	Voltage [V]	Current [A]
Coarse Sun sensor (x3)	0	0-0.09	0.035
ASTRO APS	<12	30-52	-
VST-68M	3	9-40	-
ASTRIX 1120 (x2)	13.5	22-50	-
RSI 15-215/20 (x4)	15	21 to 37	< 4.5
RMR-106F 40N (x4)	20.1	28	-

4.3 ADCS subsystem diagram

In this section a detailed subsystem architecture diagram of the ADCS subsystem and how the subsystem will be integrated with the rest of the spacecraft subsystems is presented[23].

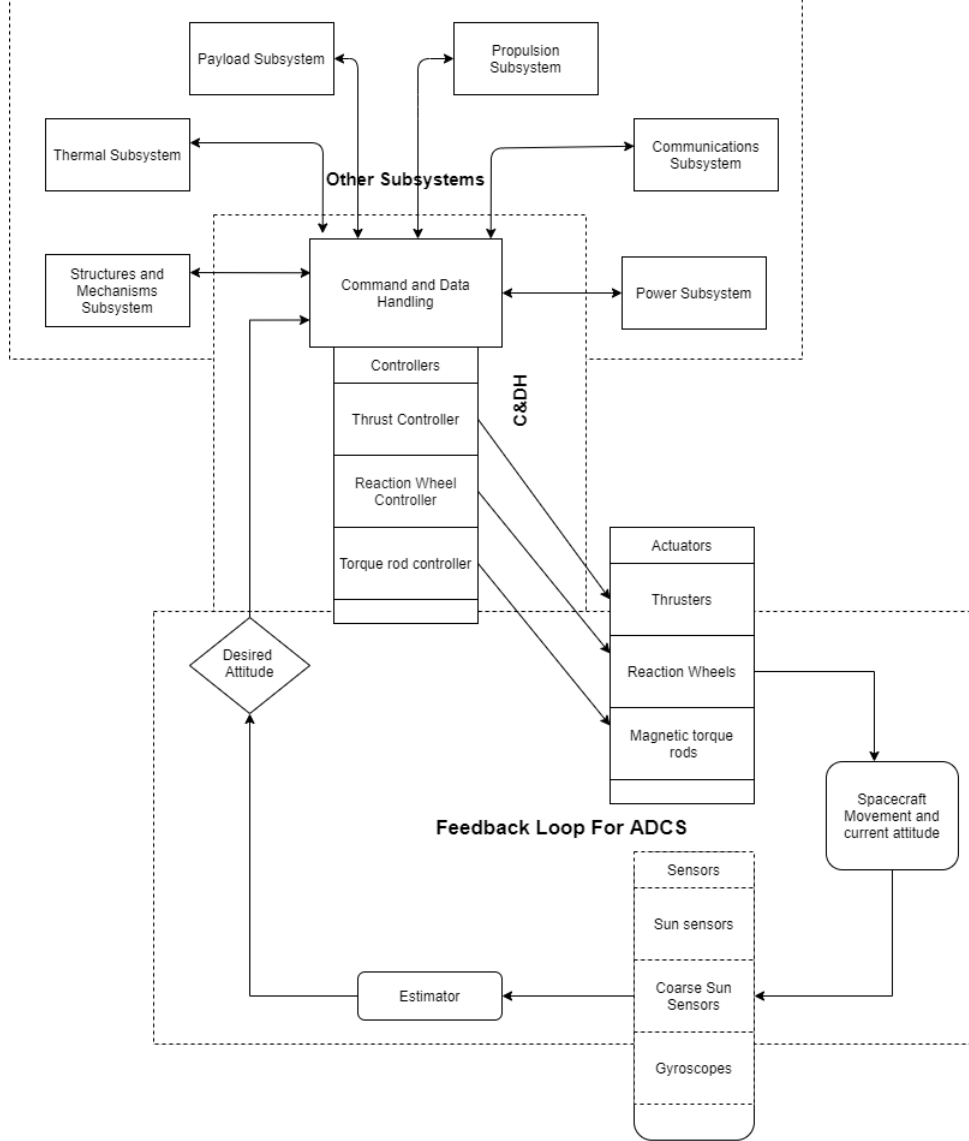


Figure 4.1: ADCS architecture diagram

As presented by Figure 4.1 a feedback information loop has been used in order for the spacecraft to actively orient its self to the required position[24]. A feedback loop for the ADCS subsystem is a process in which the sensors measure the spacecrafts attitude and provides input that compares the current attitude to the desired attitude. The difference between the current attitude and the desired attitude is known as the attitude error which is then input into the controller, consequently, the controller calculates the required torque by the actuator in order to get as close to the desired altitude as possible, and finally, the results of the torque produced by the actuator updates the current spacecraft movement and attitude. This while process is repeated in a loop in order for the spacecraft to update its position constantly depending on the required attitude.[25]

Conclusion 5

The aim of this report is to describe the design process for the ADCS subsystem of the JUICE mission. This was done in different steps. First a search was conducted on three potential types of control actuators and three control actuators to be used for attitude control, along with listing their technical specification such as dimensions, mass and power consumption. Then, calculations were performed for estimating the different types of torques experienced by the spacecraft and the various configurations possible for attitude control were determined. A trade off was then performed between the configurations to find the one that suited the mission the best. A CATIA kinematic model was also implemented, showing how the actuators help overcome the disturbance forces. Finally, the ADCS needs to be integrated with the rest of the spacecraft.

Different ADCS sensors and actuators are available on the market. Various models were analyzed: three star sensors, two gyroscopes, three thrusters for momentum dumping, a momentum wheel and a Control Moment Gyros. Then, the different torques acting on the spacecraft were determined for each phase of the mission. When near the Sun, the spacecraft experiences a torque of $3.54 \cdot 10^{-5} Nm$. When orbiting Jupiter the planet's magnetic field will cause a torque of $5.85 \cdot 10^{-4} Nm$ and its gravity field one of $3.62 \cdot 10^{-4} Nm$. To counteract these disturbance torques the reaction wheels need to generate a torque of $2.867 \cdot 10^{-3} Nm$ and the thrusters one of $120 Nm$.

Among the different proposed configurations for sensors and actuators a trade off was performed, which led to choosing configurations S2 with three coarse sun sensors, two star sensors and six gyroscopes. The sun sensors needs to be placed on the three axes of the spacecraft and they need unobstructed view of the Sun, the star sensors are going to be mounted orthogonal with respect to each other and they need unobstructed view of the sky as well. Configuration A1 was selected for actuators, consisting of four momentum wheels and four RCS thrusters.

Each of the sensor and actuator used on board is going to need power in order to operate properly. The power consumption of each component is listed in Table 5.1

Table 5.1: Power consumption of sensors and actuators

Sensor or actuator	Power [W]	Voltage [V]	Current [A]
Coarse Sun sensor (x3)	0	0-0.09	0.035
ASTRO APS	<12	30-52	-
VST-68M	3	9-40	-
ASTRIX 1120 (x2)	13.5	22-50	-
RSI 15-215/20 (x4)	15	21 to 37	< 4.5
RMR-106F 40N (x4)	20.1	28	-

References

- [1] B. Space. (2020). Bradford - coarse sun sensor, [Online]. Available: <https://www.bradford-space.com/products-aocs-coarse-sun-sensors.php>.
- [2] ——, (2020). Bradford - fine sun sensor, [Online]. Available: <https://www.bradford-space.com/products-aocs-fine-sun-sensors.php>.
- [3] Sodern. (2020). Sodern - std 15, [Online]. Available: <https://satcatalog.com/datasheet/Sodern%5C%20-%5C%20STD%5C%2015.pdf>.
- [4] Jena-Optronik. (2020). Astro aps - star sensor - jena optronik, [Online]. Available: <https://www.jena-optronik.de/products/star-sensors/astro-aps.html>.
- [5] V. Aerospace. (2020). Star trackers - vectronic aerospace, [Online]. Available: <https://www.vectronic-aerospace.com/star-trackers/>.
- [6] Jena-Optronik. (2020). Astro aps - star sensor - jena optronik, [Online]. Available: <https://www.jena-optronik.de/products/star-sensors/star-sensor-astro-15.html>.
- [7] F. of Aerospace Engineering, *Aerospace Design & Systems Engineering Elements I Part: Spacecraft (bus) Design and Sizing*. TU Delft, 2020.
- [8] AIRBUS. (2018). Astrix® 1000 series, [Online]. Available: <https://satcatalog.com/datasheet/Airbus>.
- [9] L. H. Corporation. (). Cirrus & cirrus ex — compact inertial reference units for space, [Online]. Available: <https://satcatalog.com/datasheet/L3Harris>.
- [10] A. Rocketdyne, *In-space propulsion data sheets*, <https://www.rocket.com/sites/default/files/documents/In-Space%20Data%20Sheets%204.8.20.pdf>, 2020.
- [11] MOOG, *Propulsion / monopropellant thrusters*, <https://satcatalog.com/datasheet/MOOG%20-%20MONARC-5.pdf>, 2018.
- [12] R. Collins. (2007). Rsi 45 momentum and reaction wheels 15 – 45 nms with integrated wheel drive electronics, [Online]. Available: <https://satcatalog.com/datasheet/Collins%5C%20Aerospace%5C%20-%5C%20RSI%5C%2015-215-20.pdf>.
- [13] B. Zandbergen, *AE1222-II: Aerospace Design & Systems Engineering Elements I*.
- [14] Airbus. (2020). Cmg 40-60 s, [Online]. Available: <https://satcatalog.com/datasheet/Airbus%5C%20-%5C%20CMG%5C%2040-60S.pdf>.
- [15] S. Interplanetary. (). Microsatellite torque rods, [Online]. Available: <https://satcatalog.com/datasheet/Airbus%5C%20-%5C%20CMG%5C%2040-60S.pdf>.
- [16] B. group, *Initial sizing of the juice spacecraft*, 2020.
- [17] M. WITZMANN. (). How to (iii): Calculate satellite disturbance torques, [Online]. Available: <https://www.validspace.com/how-to-calculate-satellite-disturbance-torques/>.
- [18] C. E. Eyerman, “Ta systems engineering approach to disturbance minimization for spacecraft utilizing controlled structures technology”, 2020.
- [19] R. Noomen. (). Flight and orbital mechanics, [Online]. Available: https://ocw.tudelft.nl/wp-content/uploads/AE2104-Orbital-Mechanics-Slides_9.pdf.

- [20] (2020). Apollo 11, [Online]. Available: https://en.wikipedia.org/w/index.php?title=Apollo_11&action=history.
- [21] B. group, *Design of the juice spacecraft*, 2020.
- [22] T. Space. (). Power conditioning and distribution unit, [Online]. Available: https://www.terma.com/media/177707/power_conditioning_and_distribution_unit.pdf.
- [23] P. Z. S. D. A. Spencer, *Development of an integrated spacecraft guidance, navigation, control subsystem for automated proximity operations*, 2015.
- [24] A. S. Engineering, *Attitude determination and control*, 2020.
- [25] M. A. B. P.E., *Spacecraft subsystems part 1 - fundamentals of attitude control*, 2015.

CATIA Drawings A

In this appendix the CATIA Drawings are given for different configuration options.

A.1 Configuration S1 and A1

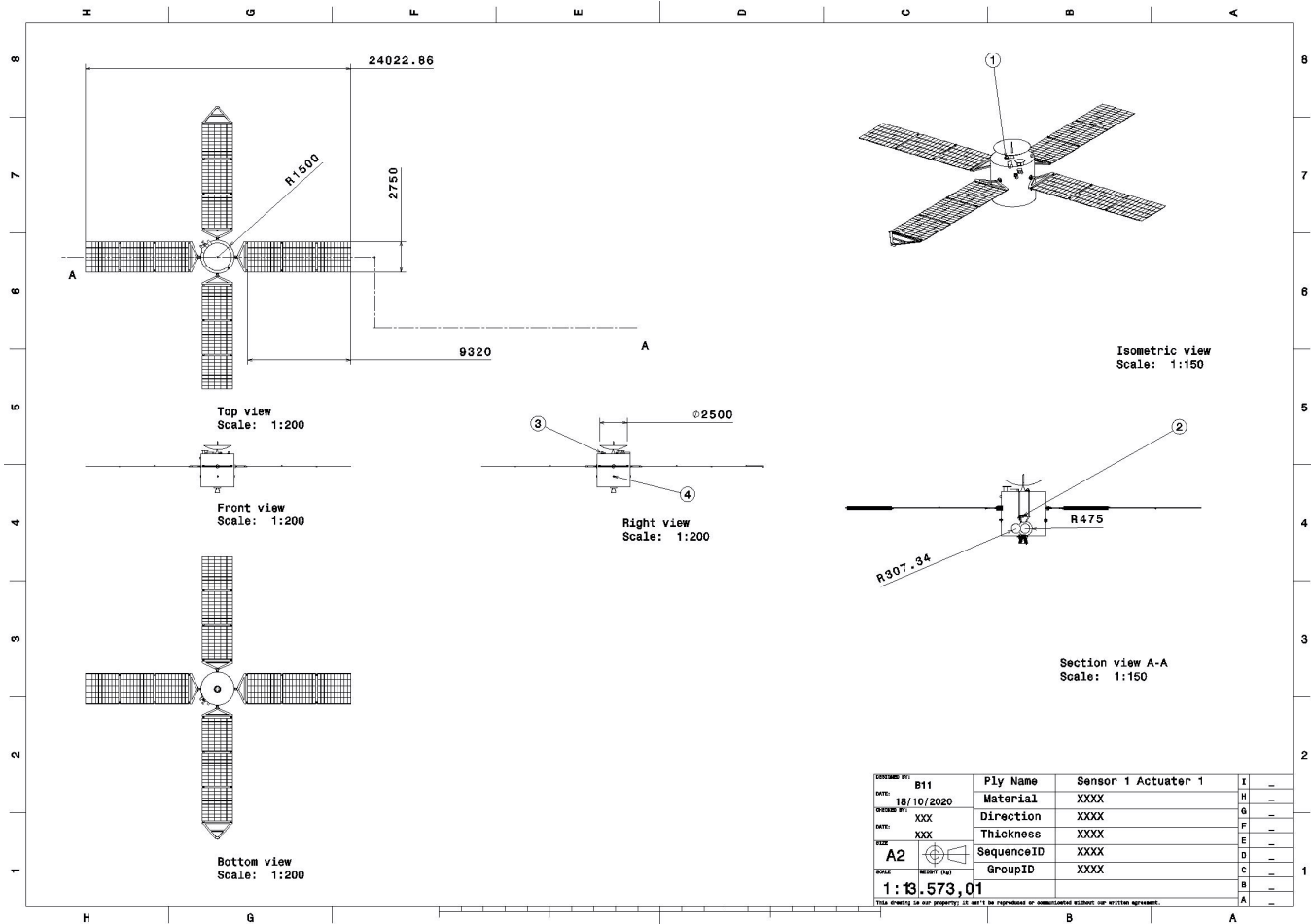


Figure A.1: Configuration S1 and A1

Table A.1: Part list S1 and A1

Part Number	Part Name	Quantity
1	ASTRIX 1120	1
2	RSI 15-215/20	4
3	ASTRO APS	1
4	MRM-106F	4

A.2 Configuration S3 and A2

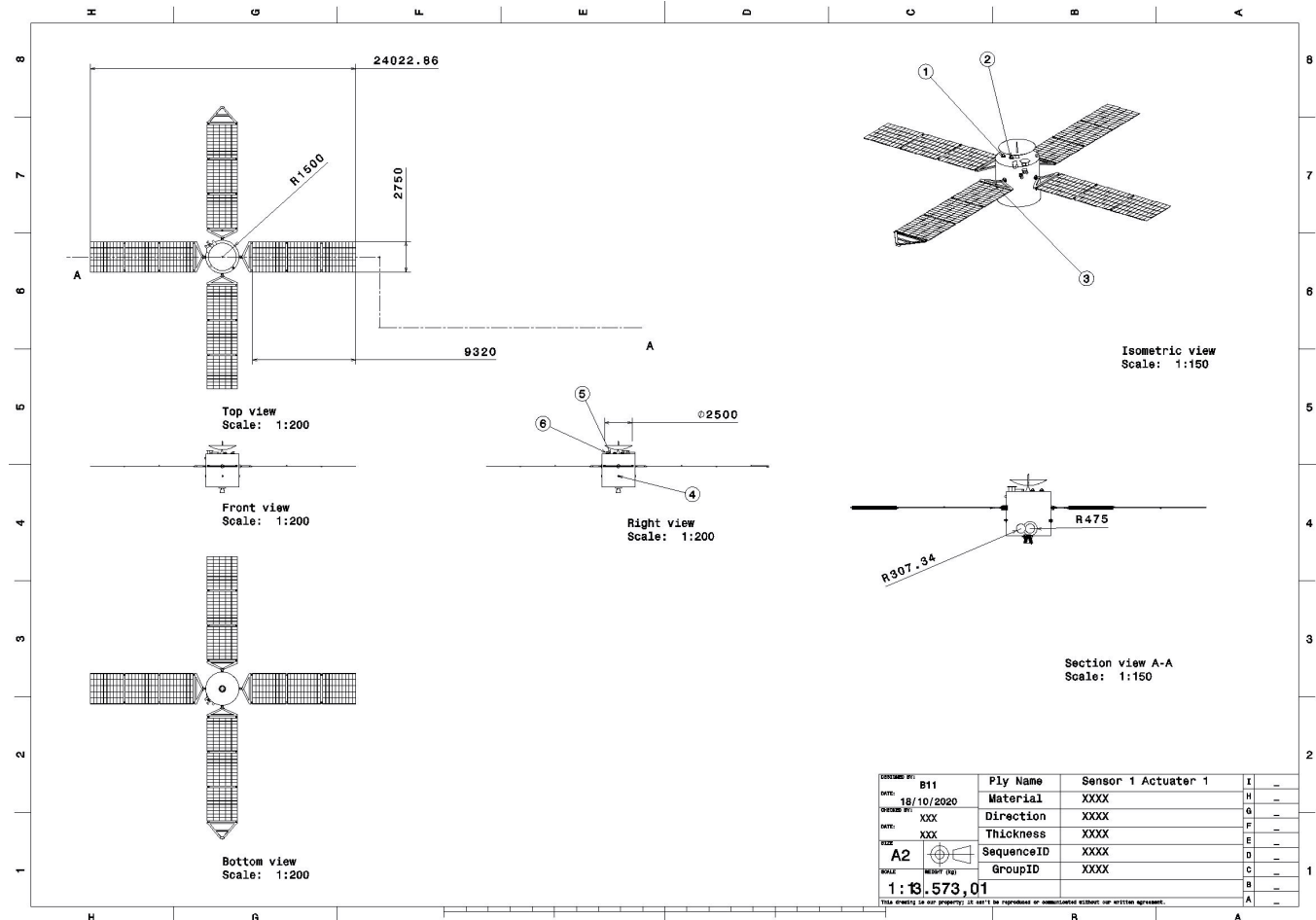


Figure A.2: Configuration S3 and A2

Table A.2: Part list S3 and A2

Part Number	Part Name	Quantity
1	ASTRIX 1120	2
2	CMG 40-60S	4
3	Fine Sun Sensor	1
4	MONARC-5	24
5	ASTRO APS	1
6	Horizon Sensor	1

A. CATIA DRAWINGS

A.3 Configuration S2 and A1 with the other Components

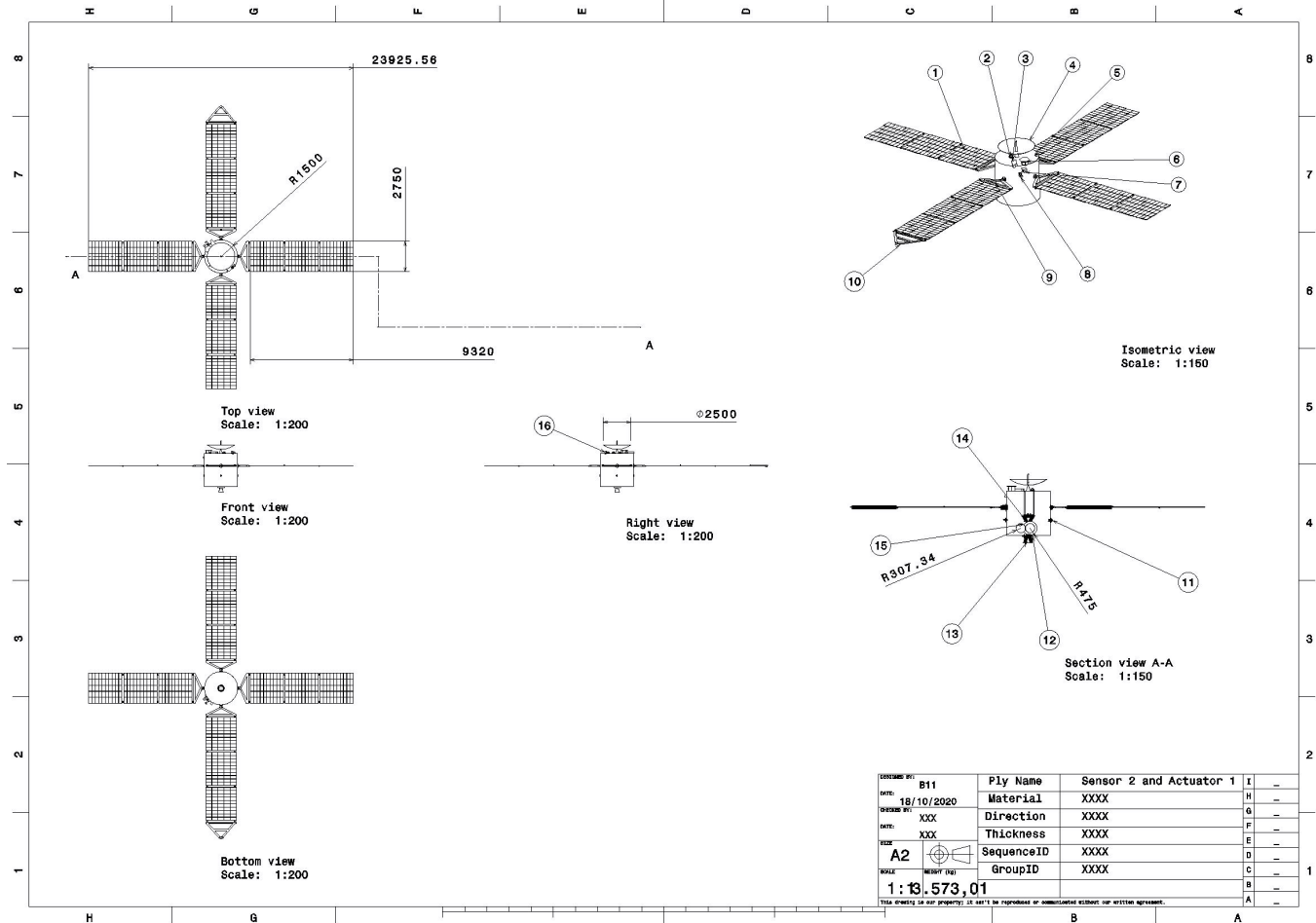


Figure A.3: Configuration S2 and A1

Table A.3: Part list S2 and A1

Part Number	Part Name	Quantity
1	Solar Panel	4
2	ASTRIX 1120	2
3	UVS	1
4	Antenna	1
5	Battery	1
6	JIRAM	1
7	CAPS	1
8	JunoCam	1
9	Course Sun Sensor	3
10	MAG	1
11	MRM-106F	4
12	Debris Shield	1
13	Leros 1B	1
14	RSI 15-215/20	4
15	Propellant Tanks	3
16	ASTRO APS	1
16	VST-41M	1

A.4 Configuration S4 and A3 with the other Components

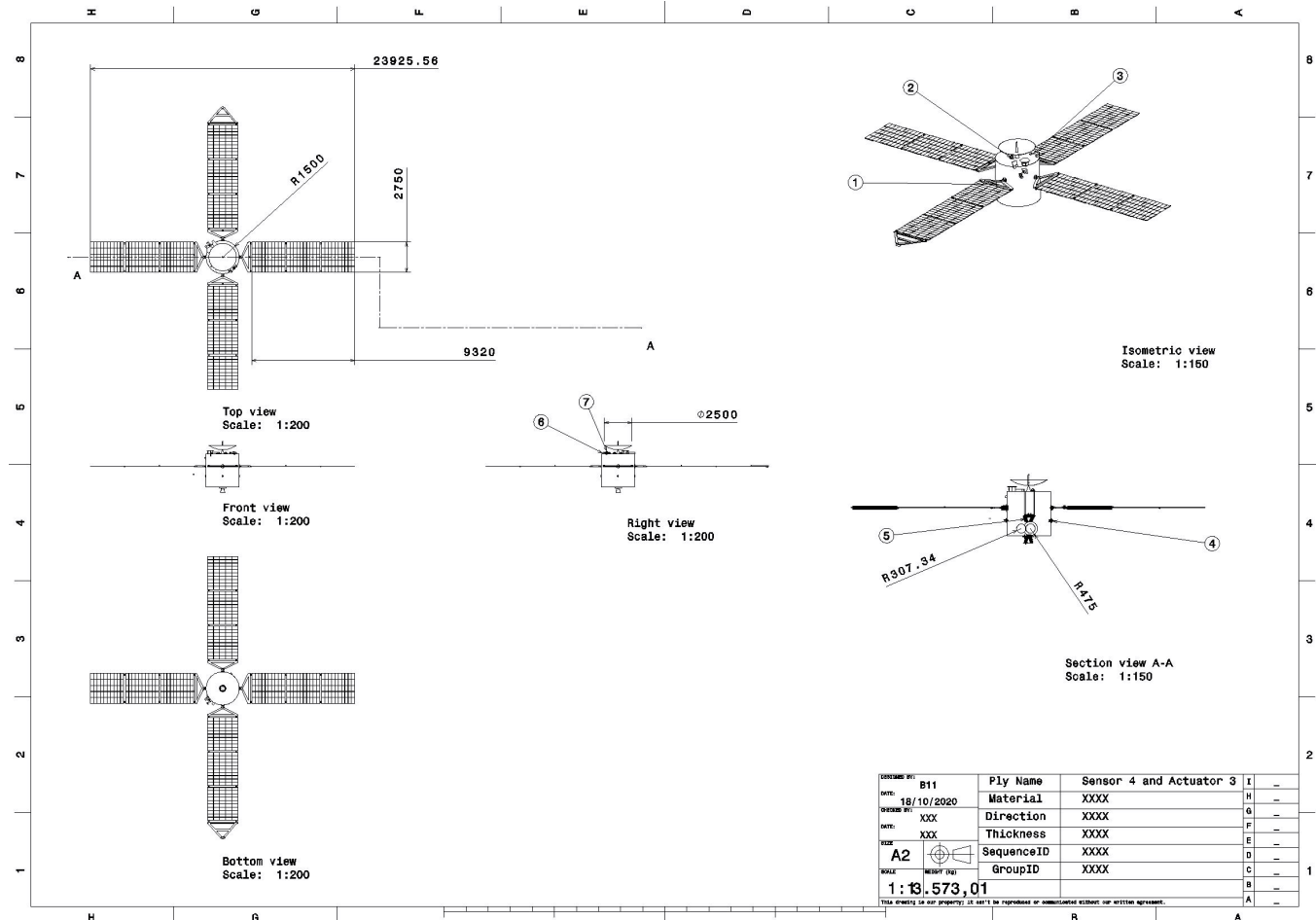


Figure A.4: Configuration S4 and A3

Table A.4: Part list S4 and A3

Part Number	Part Name	Quantity
1	Sun Sensor	8
2	ASTRIX 1120	2
3	QT-40	3
4	MONARC-5	12
5	RSI 15-215/2	4
6	ASTRO 15	2
7	VST-68M	1

Task Distribution B

In this appendix, Table B.1 presents the task distribution among the different team members.

Table B.1: Task distribution per member

Deliverables	Members
D3.1.1	Niklas, Lorenz, Stefano, Jonatan
D3.1.2	Tarek, Silvano, Sam, Antonio
D3.1.3	Lorenz, Jonatan
D3.2.1	Niklas
D3.2.2	Jonatan
D3.3.1	Silvano
D3.3.2	Stefano, Sam
D3.3.3	Tarek
Summary	Sam
Introduction	Antonio
Conclusion	Antonio
Proof reading	Stefano

As compensation for the hour that was missed by Tarek in the project session, an hour was spent outside project hours working on the actuator effects during the mission timeline.